



Time distributions of solar energetic particle events: Are SEPEs really random?

P. T. A. Jiggins¹ and S. B. Gabriel¹

Received 27 March 2009; revised 26 May 2009; accepted 27 June 2009; published 16 October 2009.

[1] Solar energetic particle events (SEPEs) can exhibit flux increases of several orders of magnitude over background levels and have always been considered to be random in nature in statistical models with no dependence of any one event on the occurrence of previous events. We examine whether this assumption of randomness in time is correct. Engineering modeling of SEPEs is important to enable reliable and efficient design of both Earth-orbiting and interplanetary spacecraft and future manned missions to Mars and the Moon. All existing engineering models assume that the frequency of SEPEs follows a Poisson process. We present analysis of the event waiting times using alternative distributions described by Lévy and time-dependent Poisson processes and compared these with the usual Poisson distribution. The results show significant deviation from a Poisson process and indicate that the underlying physical processes might be more closely related to a Lévy-type process, suggesting that there is some inherent “memory” in the system. Inherent Poisson assumptions of stationarity and event independence are investigated, and it appears that they do not hold and can be dependent upon the event definition used. SEPEs appear to have some memory indicating that events are not completely random with activity levels varying even during solar active periods and are characterized by clusters of events. This could have significant ramifications for engineering models of the SEP environment, and it is recommended that current statistical engineering models of the SEP environment should be modified to incorporate long-term event dependency and short-term system memory.

Citation: Jiggins, P. T. A., and S. B. Gabriel (2009), Time distributions of solar energetic particle events: Are SEPEs really random?, *J. Geophys. Res.*, *114*, A10105, doi:10.1029/2009JA014291.

1. Introduction

[2] Energetic particles originating from the Sun are contained in relatively short bursts called Solar Energetic Particle Events (SEPEs). Effects on spacecraft from SEPEs include ionization, displacement damage, sensor background noise, damage to biological systems, single event effects and they could also be hazardous to humans especially those on deep space missions in the future [*Feynman and Gabriel*, 2000]. Aircraft and even ground-based systems can also be affected by Solar Energetic Particles (SEPs) in some severe cases such as the “Halloween Events” during October and November 2003 [*Dyer et al.*, 2004].

[3] The largest of these SEPEs are characterized by a large enhancement in the flux of protons of energies from a few MeV to GeV levels at 1 AU and are therefore sometimes known as solar proton events (SPEs). These events are easily detected as the flux increases from a background level less than 1 particle $\text{cm}^{-2} \text{ster}^{-1} \text{s}^{-1}$ (or particle flux units (pfu)) in the >10 MeV energy range to tens, hundreds, thousands and

even tens of thousands of pfu. Prior to arrival at the Earth particles must first propagate through the interplanetary medium, the first protons may arrive within hours [*Krucker and Lin*, 2000] although some high-energy particles have been measured within 15 min of an event being observed [*Mewaldt et al.*, 2005].

[4] For over 40 years it was believed that solar flares were the sole cause of SEPEs but it is now accepted that this is not the case, this is termed “the solar flare myth” [*Gosling*, 1993]. The current paradigm is that there are two types of SEPEs: smaller, low-fluence, short-duration (or impulsive) events caused by solar flares and larger, high-fluence, longer-duration (or gradual) events accelerated in coronal/interplanetary shocks driven by coronal mass ejections (CMEs). Two differences between impulsive and gradual events are the height in the corona at which the particles can be said to be initiated and the respective volumes. Impulsive events occur in the corona at a height of <10⁴ km and have a total volume generally in the region of 10²⁶–10²⁸ cm³ while gradual events occur in the corona at a height of ~5 × 10⁴ km and have a total volume generally in the region of 10²⁸–10²⁹ cm³ [*Kallenrode*, 2003]. A review of the different particle acceleration mechanisms and resulting particle compositions from CME-driven shocks and solar flares was given by *Reames* [1999, and references therein]. It is now widely thought that CMEs

¹Astronautics Research Group, University of Southampton, Southampton, UK.

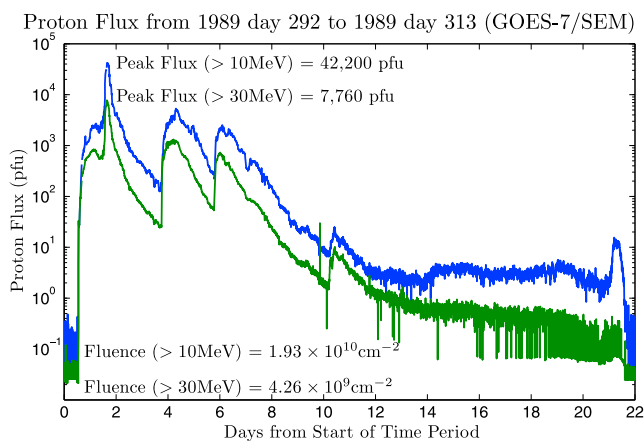


Figure 1. Event flux profile for the large October 1989 event resulting from multiple CMEs.

produce the major transient disturbances in the near-Earth space environment [Kahler, 2003]. However, recent observations of mixed events suggest that this two-class division of SEPES needs to be modified [Kallenrode, 2003].

[5] The size and risetime to the peak flux of an event depend on the position of the source phenomenon on the solar surface with a tendency for those events resulting from activity on the Sun’s western hemisphere to be larger and have faster risetimes reflecting the connection of the magnetic field line from the Earth to a point on the Sun in this region [Lario *et al.*, 2006]. SEPES extending to the highest energies result in Ground Level Enhancements (GLEs) and are caused by CMEs which are usually faster and wider than those causing smaller events [Wang and Wang, 2004]. However, although it is known that the CME speed and SEP intensity are correlated, for a given CME speed SEP intensity can vary over 4 orders of magnitude [Gopalswamy *et al.*, 2003]. Following the peak there is the decay phase of the event as the flux returns to the background level. Events caused by a single CME can have durations from several hours to several days [Reames, 2004].

[6] Major historical SEPES recorded include: the event of 23 February 1956 which was particularly notable for having a very hard spectrum [Mewaldt *et al.*, 2005], the “Carrington Event” of September 1859 [Carrington, 1860] which is recognized as the largest event of the past 450 years [Shea *et al.*, 2006], the August 1972 event which dominated solar cycle 20 [King, 1974] and the October 1989 event which is the largest well-recorded particle event so far [Kallenrode and Cliver, 2001]. The flux profiles for the October 1989 event from the GOES 7/SEM >10 MeV and >30 MeV channels are shown in Figure 1. It can clearly be seen that there are multiple increases caused by multiple CMEs but for the remainder of this article such sequences (which can last as long as a month) will be considered a single event.

[7] For modeling the statistics of the SEP environment it is standard to link consecutive enhancements where the flux does not return to the background level between events. Tylka *et al.* [1997] termed these “episodes” and highlighted that a modeling technique which ignored an obvious correlation between enhancements would systematically underpredict the probability of such a sequence of events. Those studying the physics and creating physical models of SEPES often refer to such a sequence as compound events while a

single enhancement would be referred to as an isolated event (one example use of this terminology is that by Ho *et al.* [2003]). Kuznetsov *et al.* [2005] opposed the view that multiple enhancements should be considered a single event stating that each of the occurrences must be regarded as resulting from a certain single process originating on the Sun.

[8] The event lists used in this study all seek to link connected SEPES in the way highlighted by Tylka *et al.* [1997] albeit through different methods. Defining events in this way mitigates factors such as the effect of a seed population in the interplanetary medium resulting from one CME then being accelerated by a shock from a future CME [Reinard and Andrews, 2006] and CME interaction [Gopalswamy *et al.*, 2002] both of which can affect the size (peak flux, fluence, etc.) of the SEPES.

[9] As we use a single time series of proton flux data recorded at 1 AU it is not always possible to separate contributions from different physical processes on the solar surface. The three separate event lists (JPL, PSYCHIC and NOAA) used in this study each have different event definitions and therefore on occasion treat a series of enhancements differently as one or more events. By taking these independently created event lists we test the robustness of the distributions fitted and sensitivity to different treatment of episodes (or compound events).

[10] Enhancements can appear very differently at different helioradial distances, a good example of this using electron data from Helios 1 and IMP 8 is given by Cane [2005, Figure 6]. However, using our definition of an event, which combines such sequences (applied to the electron fluxes) both would be classified as only 1 event as the flux does not return to the background level in between enhancements. We have only shown that the distributions are applicable at 1 AU, they may or may not be applicable at other helioradial distances but this cannot be determined without further data and are certainly not applicable for physical process (i.e., flares and CMEs that give rise to SEPES) on the surface of the Sun.

[11] By identifying these enhancements in the flux time series a list of events is produced and a statistical distribution found to model the frequency of these events. This distribution, in conjunction with the event characteristics (fluence, peak flux and duration), can then be used to predict the SEP environment for the future. It was shown by Feynman *et al.* [1990] that the 11-year solar cycle can be split into an approximately 4-year quiet period and a 7-year active period and that the fluence contribution from the quiet periods was negligible in comparison to the active years. However, recently there has been interest in models for solar minimum [Xapsos *et al.*, 2004] which does include some events such as those in December 2006 [Myagkova *et al.*, 2009]. For this reason in this study we investigate both the complete time period and the time period including only solar maximum years. The active year periods are assumed to begin 2.5 years before and end 4.5 years after the date of peak sunspot number for that solar cycle. These maxima are taken to be 1968.9, 1979.9, 1989.9 and 2000.2 for cycles 20–23 [Xapsos *et al.*, 2004].

[12] Currently all established models for the SEP environment [King, 1974; Feynman *et al.*, 1993; Nymmik, 1999; Xapsos *et al.*, 1998, 1999, 2000, 2004] assume a Poisson distribution to model the frequency of SEPES. The JPL 91

model for cumulative mission fluence [Feynman et al., 1993] employs such a Poisson distribution combined with a Monte Carlo method and a lognormal distribution to generate event fluences. Nymmik [1999], in the creation of the MSU model, suggested that the event frequency is related to the sunspot number proxy for solar activity. This proxy gives an average event rate which is then input into the Poisson distribution and combined with a modified power law to calculate event fluences. The link between event frequency and sunspot number has been questioned by Feynman et al. [2002] due to a low correlation coefficient of 0.6 between the two. Combined with the difficulty in reliably predicting the future sunspot number this technique is very difficult to justify. The ESP (Emission of Solar Protons) cumulative fluence model [Xapsos et al., 2000] is based purely on the yearly fluence fitted with a lognormal distribution assuming that events are Poisson distributed and therefore the result for 1-year fluence can be extrapolated to different mission lengths using simple formulae. Related models for worst case event flux [Xapsos et al., 1998] and worst case event fluence [Xapsos et al., 1999] also use a Poisson assumption to obtain their results.

[13] The Poisson distribution has two major requirements to be applicable: the rate of events must be invariant with time (i.e., the process should be stationary) and the activity of the past should have no impact on the likelihood of a future event (i.e., the system should have no “memory” or each event is independent of the previous one). In this paper we focus on the waiting times between events which are related to the event frequency (being the transform from the frequency domain into the time domain) and the event durations which are one characteristic of events. We examine the assumptions of stationarity of the process and independence of consecutive events and propose two possible alternatives to the Poisson distribution for modeling event frequency and durations namely a time-dependent Poisson distribution and the Lévy distribution. We find that there is memory existing in the process despite efforts to define events in a way that ensures consecutive events are independent and that the process, rather than being stationary, has a long-term time dependence which is not linked to solar cycle variation. In effect, SEP event occurrences are not random in time but are dependent on recent activity and longer-term changes in the Sun even within solar active periods. We show that the Poisson process is inadequate to describe the behavior of SEPES and that this will impact assumptions and outputs of existing statistical models used for engineering design purposes.

2. Data Sets and Event Lists

[14] In the literature there have been various definitions of events using different parameters to extract the events from the time series: the energy level, the flux threshold, the time after the event drops below the threshold before it is said to have ended (we call this the lag time), the sampling time (i.e., the time binning of the time series) and the minimum event characteristics (such as the lowest fluence of event considered [Feynman et al., 1993; Xapsos et al., 1999] or the lowest peak flux of event considered [Xapsos et al., 2004]).

[15] The flux thresholds are chosen to distinguish the events from the background and are varied with the energy

channel selected (the starting and ending thresholds are most commonly chosen to be the same). Combined with the lag time these thresholds also serve to link connected events where there may be a causal link between consecutive CMEs [Tylka et al., 1997].

[16] The minimum sampling time is the time resolution of the instrument being used, using this gives the most accurate measurements of event peak flux, start and end times and consequently event fluence. However, in order to mitigate for errors in the data often the sampling time is increased (so the effects of spikes, gaps, etc. are reduced). Feynman et al. [1990, 1993] and Jun et al. [2007] took a sampling time of 1 day. A minimum duration, peak flux or fluence can be applied to the list of events to neglect small events which might be of little consequence, more greatly affected by data errors or erroneous due to poor data. It should be noted that while these events may be excluded due to their negligible contribution to fluence or low peak flux they may be important in terms of the science and tests applied to the events waiting times.

[17] To test the robustness of the various distributions we used 3 separate event lists created using different parameters with differing aims in mind: a JPL event list using data from Feynman et al. [1990] extended using the same event parameters and GOES/SEM time series data from the >10 MeV energy channel, the PSYCHIC event list provided by M. Xapsos and the National Oceanic and Atmospheric Administration (NOAA) SEP event list.

[18] Figure 2 shows the event frequency (top plots) and mean waiting time (bottom plots) for each of the event lists, this was calculated every 6 months to clearly show the variations in time. The greater sensitivity of the PSYCHIC event definition results in a higher number of events while the JPL and NOAA definitions return similar results. Also shown the bounds of the 7-year solar active periods when there is greatly increased activity as noted by Feynman et al. [1990].

2.1. JPL Event List

[19] One model which is widely used and has seen various incarnations over the past 2 decades is the JPL model [Feynman et al., 1990, 1993, 2002]. The events were defined separately in the >10 MeV energy channel using a threshold of 1 pfu, a lag time of 2 days, a sampling time of 24 h and a minimum event fluence of 10^6 cm^{-2} [Feynman et al., 1993]. For our event list we used data from GOES/SEM instruments as shown in Table 1 to extend the event list published in the JPL 85 model for the time prior to January 1986 which used IMP and OGO data [Feynman et al., 1990] (the JPL 91 event list was not published). For the time period from 1986 we checked each of the event flux time series plots and removed those entries that were data errors rather than real events.

[20] We favored data from one spacecraft instrument compared to another based on its reported reliability [Rosenqvist et al., 2005]; this meant using GOES 7 and GOES 8 data as much as possible. Often at the ends of the data set there are a greatly increased number of data gaps so we analyzed the time series and avoided using data from time periods when the portion of gaps was above ~10%. We also cross-checked the list with the NOAA list to ensure that no major events had been missed. It includes 276 events

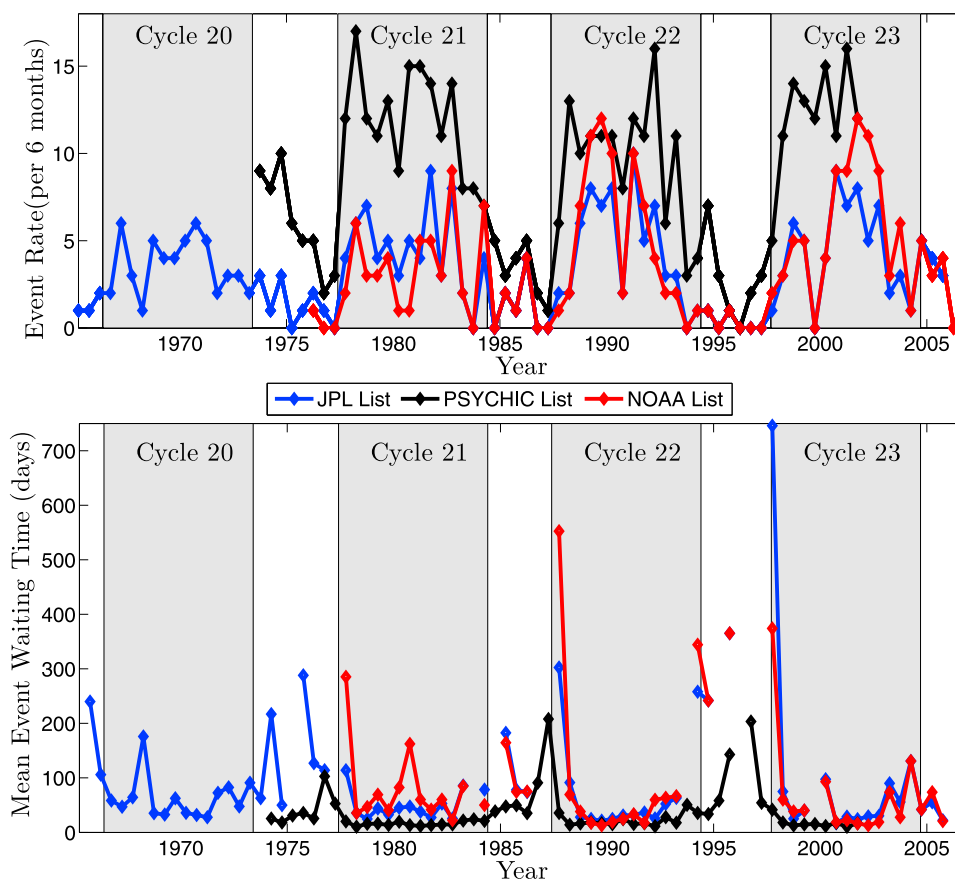


Figure 2. Plots of event rates and mean waiting times binned in 6 month periods for each event list; gaps appear in the waiting time plot where there are no events in the 6 month time period. The 7-year active period for solar cycles 20–23 are also shown.

over a 41 year time period (1965–2005). This event list used is included in Appendix A.

2.2. PSYCHIC Event List

[21] The event list used for the recent PSYCHIC model [Xapsos *et al.*, 2004] contains many more events (481) over a shorter time period of 28 years (November 1973 to November 2001) than the list generated using the JPL model event definition. It uses IMP 8/GME data supplemented with GOES/SEM data during periods of high flux to counter saturation effects and IMP 8/CPME data prior to 1986 as no GME data is available before this time. Extensive analysis has been undertaken to calibrate and combine all this data to get the best features from the different instruments [Xapsos *et al.*, 2004]. Events detected are said to begin when the flux first goes above the background and end when the flux first returns to the background. This event identification procedure was done manually. Events were then excluded if the peak differential flux in the 1.15 to 1.43 MeV channel did not exceed $>4 \text{ cm}^{-2}\text{s}^{-1}\text{sr}^{-1}\text{MeV}^{-1}$ and the peak flux in the 42.9 to 51.0 MeV channel did not exceed $>0.001 \text{ cm}^{-2}\text{s}^{-1}\text{sr}^{-1}\text{MeV}^{-1}$ [Xapsos *et al.*, 2004]. This event definition resulted in the inclusion of a larger number of events significant at low and high energies.

2.3. NOAA Event List

[22] NOAA publish an online event list at <http://www.swpc.noaa.gov/ftpd/indices/SPE.txt>. This list uses

the >10 MeV channel with data taken from the GOES spacecraft and defines the start of a SEP event to be when the flux rises above 10 pfu and the end of an event being the last time the flux was greater than or equal to 10 pfu. There is no lag time, a high temporal resolution of 5 min and a requirement of 3 consecutive at the start of the event points serves to exclude “nonevents” detected by data errors. There is no minimum event size although the high threshold filters out a significant number of smaller events. The list contains 224 events over a period of 31 years from 1976 to 2006 (which is the date of the occurrence of the last event by this definition).

[23] The NOAA event list sometimes excludes smaller events included in the JPL list due to the higher thresholds such as in 1980, close to solar maximum, where it includes only 2 events compared to 8 in the JPL list. Conversely, due to the higher threshold, the NOAA list can have a greater number of events by splitting sequences where the flux drops below its 10 pfu threshold but not the JPL list’s 1 pfu

Table 1. Instruments Used for Extension of JPL Event List

Spacecraft/Instrument	Time Period
GOES 6/SEM	1 Jan 1986 to 28 Feb 1987
GOES 7/SEM	1 Mar 1987 to 31 Dec 1995
GOES 8/SEM	1 Jan 1996 to 31 Dec 2002
GOES 10/SEM	1 Jan 2003 to 13 Jun 2003
GOES 11/SEM	14 Jun 2003 to 31 Dec 2005

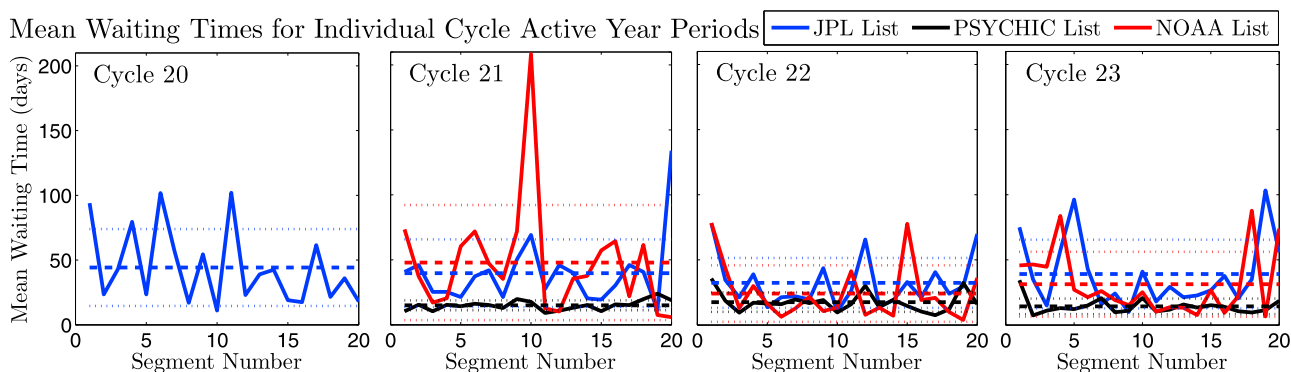


Figure 3. Binned waiting times for each cycle's active year periods with mean (dashed lines) and ± 1 standard deviation (dotted lines).

threshold. An example of this is seen in March 1989 where the JPL list has only a single event of 17 days while at that time the NOAA list has 3 separate events. Both these examples are reflected in the lists' event frequencies displayed in Figure 2 (top). This has an impact on the event waiting times and allows us to test the robustness of the distributions fitted.

3. Distributions

[24] The three functions described relate to three processes: a Poisson process, a time-dependent Poisson process and a Lévy process. The functions described here are for application in the time domain (be that event waiting time or duration) and therefore the Fourier transform of any of these functions applied to waiting time will return the probability density function (pdf) of event frequency for that process.

3.1. Poisson Process

[25] A Poisson process has been assumed in all SEPE engineering environment models up to now. On the basis of basic Poisson assumptions, the likelihood of at least one event occurring in a given time period, Δt , is given by the cumulative density function (cdf) of the exponential distribution:

$$P(> 0; \Delta t) = 1 - e^{-\lambda \Delta t} \quad (1)$$

and therefore the expression of a Poisson process in the time domain, or waiting time distribution (wtd), is equal to the pdf of the exponential distribution:

$$P(\Delta t) = \lambda e^{-\lambda \Delta t} \quad (2)$$

[26] When plotted with a logarithmic axis of ordinates, equation (2) will be a straight line with intercept $\ln(\lambda)$. *Feynman et al.* [2002, Figure 5] produced a plot of binned waiting times against the relative number with a straight line fit in support of the events following a Poisson process. In the frequency domain the likelihood of seeing k events in a fixed time period, T , is given by

$$P(k, T) = \frac{e^{-\lambda T} (\lambda T)^k}{k!} \quad (3)$$

where λ is the mean number of events per day.

[27] Crucial features of a Poisson process is that the likelihood of an event occurring in a coming time period

is not affected by recent activity (i.e., the process has no memory) and the mean rate of event occurrence, λ , does not vary with time; that is, the process is stationary. The first of these factors can be seen as the absence of a short-term time dependence while the second can be seen as the absence of a longer-term time dependence.

3.2. Stationarity

[28] For the process to be stationary the mean waiting time should be independent of time. To test stationarity the events' waiting times were grouped into 20 segments each of which had the same number of events (and therefore varied in real time covered). The mean waiting time is then calculated for each segment. If the events in the active year periods can be considered to be governed by a Poisson process then there should be little variability and certainly no trend. The greater the scatter is, the less stable the mean value will be. If the waiting time segments have high scatter this indicates periods of high waiting times (low activity) and periods of low waiting times (high activity) within the selected time period.

[29] The mean waiting times per 6 months shown in Figure 2 (bottom) indicate a lower variation in waiting times for the PSYCHIC list compared to the JPL and NOAA lists due to a lower absolute value for the mean waiting time and hence lower absolute variation. The grouped waiting time for active years for the individual cycles (20–23) with the mean and ± 1 standard deviation are plotted in Figure 3, the characteristics are shown in Table 2. It is clear that the waiting times for the PSYCHIC list are consistently lower which is to be expected as the list includes far more events. It is also apparent that the JPL and NOAA lists have a greater degree of scatter characterized by a far higher standard deviation. It is possible that some of this scatter is as a result of a low number of events in each bin (notably for the NOAA list in cycle 21 where each bin had only 2 events). When we investigate the mean and standard deviation for 20 segments for the joined active year periods so that each segment includes far more events (Figure 4, bottom), we find a very similar trend. The plot of the complete time period (Figure 4, top) shows higher mean values and higher standard deviations as the process is not stationary when the quiet years are included as noted by *Feynman et al.* [1990].

[30] To test the theory that the mean value is not stationary within reasonable parameters we use a bootstrap method.

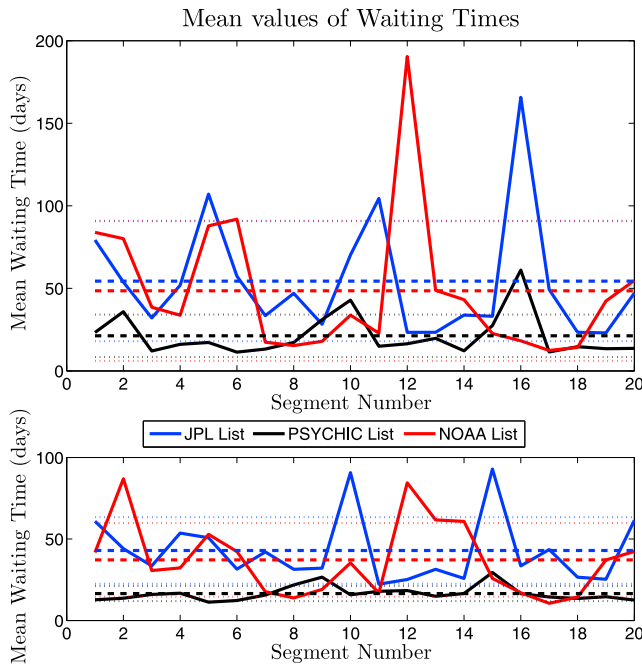


Figure 4. Binned waiting times for (top) the total time period and (bottom) the joined active year periods with mean (dashed lines) and ± 1 standard deviation (dotted lines).

By randomizing the waiting times we create a virtual time line with 20 new time segments. The mean of the segments is necessarily the same but the standard deviation will vary. By carrying out 10,000 iterations we compare the real time line standard deviations to the virtual ones where we know the waiting times are randomized. With this comparison we can test the null hypothesis that the process is stationary. Table 3 shows the mean waiting time, the standard deviation between the 20 time segments in the real time line, the percentage of virtual time lines with a higher standard deviation and the number of events in each segment for both the complete time period and the joined active year waiting times.

[31] The complete time period here operates as a test for the procedure as we knew that there is a difference between the solar active and quiet years which is reflected in the rejection of the null hypothesis at the 99% confidence level in all cases. For the active years we can see that in all cases we are able to reject the null hypothesis that the process is stationary at the 95% level and in all but the NOAA case we can reject it at the 99% level. These results are a clear indication that the process is not stationary or completely random and encourage us to find a distribution which does not require the process to be stationary and instead allows the mean event rate to vary.

Table 2. Analysis of Mean Waiting Times in 20 Equal Segments for Cycles 20–23 Active Years, All Active Years, and the Complete Event Lists

Event List	Parameter	Cycle 20	Cycle 21	Cycle 22	Cycle 23	Active Years	All Years
JPL	Mean	44.2243	39.7150	32.3500	39.1456	42.9266	54.3538
	SD	29.6817	26.0690	19.1311	26.3285	20.4230	36.3146
PSYCHIC	Mean	-	15.0001	17.5501	14.3000	16.5475	21.2604
	SD	-	3.8044	7.4645	5.9406	4.6360	12.8108
NOAA	Mean	-	47.9050	24.1576	31.2977	37.1717	48.5109
	SD	-	44.2738	21.6593	24.9206	22.5887	42.4299

Table 3. Assessment of Stationarity of Event Waiting Times in the Complete Time Period and Solar Active Years Only

	Mean Waiting Time (days)	Standard Deviation (days)	Percent of Virtual Time Lines Higher	Events per Segment
<i>Complete Time Period</i>				
JPL	54.3538	36.3146	0.02	13
PSYCHIC	21.2604	12.8108	0.00	24
NOAA	48.5109	42.4299	0.03	11
<i>Active Years Only</i>				
JPL	42.9266	20.4230	0.12	12
PSYCHIC	16.5475	4.6360	0.05	20
NOAA	37.1717	22.5887	1.05	10

3.3. Time-Dependent Poisson Process

[32] It was found that a time-dependent Poisson process can be fit to the waiting times of solar flares [Wheatland, 2000] and CMEs [Wheatland, 2003]. Here it is assumed that locally the process will be Poissonian but that over time the mean rate of event occurrence is allowed to change. For a piecewise solution the wtd is given by

$$P(\Delta t) = \frac{1}{\varrho} \int_0^{\infty} P(k) k^2 e^{-k\Delta t} dk \quad (4)$$

where $P(k)dk$ is the fraction of time at a specific mean event rate (and therefore the probability of seeing that event rate) in the range of $(k, k + dk)$ and ϱ is the mean event rate for the complete event list. It was found that the mean rate (of flares, CMEs or in this case SEPES) can be approximated by an exponential distribution:

$$P(k) = \varrho^{-1} \exp(-k/\varrho) \quad (5)$$

[33] Together with a local Poisson assumption this results in a combination of two exponential distributions. When equation (5) is substituted into equation (4) and the integral evaluated we find the waiting time of events is given by

$$P(\Delta t) = \frac{2\varrho}{(1 + \varrho\Delta t)^3} \quad (6)$$

[34] This function follows power law behavior at high waiting times but deviates from it at lower waiting times predicting fewer low-waiting time events than a simple power law.

[35] Using the 6 month binned event frequencies (shown in Figure 2) and the mean values of event frequency from the sample we can compare the data to the idealized pdf's for the Poisson and time-dependent Poisson processes (Figure 5). Again there is significant scatter on the plots as a result of limited data but we can see that for active

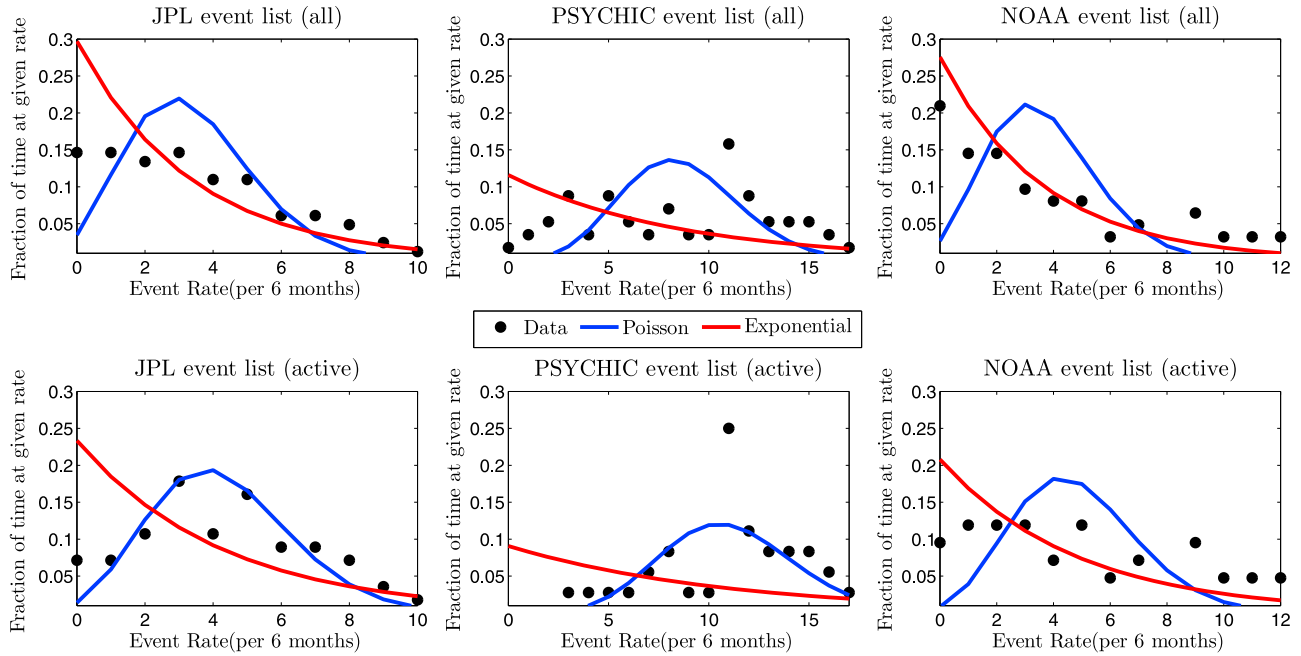


Figure 5. Event rates compared with idealized Poisson and time-dependent Poisson predictions.

years the PSYCHIC event list is well fit by the Poisson distribution while the NOAA event list is better fit by the exponential distribution. This is what we would expect given the relative stationarity of each event list found in section 3.2.

[36] The complete time period in each case is poorly fit by the Poisson distribution and there is an improvement in all cases when we consider only the active years which follows from the distinct separation of quiet and active years noted by *Feynman et al.* [1990]. The JPL list for the active years is better fit by the Poisson distribution which is surprising given the apparent lack of stationarity shown in section 3.2. It should be noted that if the process is not stationary it does not mean that the rates will be exponentially distributed, however, the final form of a truncated power law may still fit the waiting time data well.

3.4. Test for Local Poisson Distribution

[37] Both the Poisson distribution and the time-dependent Poisson distribution assume that consecutive events are independent of each other; that is, it is has no memory. To test this assumption we follow the formalism of *Bi et al.* [1989] applied to the absorption lines of a quasar which has since been applied to solar flares by *Lepreti et al.* [2001].

[38] First, the lower of the two waiting times either side of each event is found (δt). If δt is the waiting time before the event $\delta \tau$ becomes the waiting time between the two events before the original event, if it is the event waiting time after the event $\delta \tau$ becomes the waiting time between the two events after the original event:

$$\begin{aligned} \delta t_i &= \min\{t_{i+1} - t_i, t_i - t_{i-1}\} \\ \delta \tau_i &= t_{i+2} - t_{i+1} \text{ if } \delta t_i = t_{i+1} - t_i \text{ or} \\ &= t_{i-1} - t_{i-2} \text{ if } \delta t_i = t_i - t_{i-1} \end{aligned}$$

The resulting distributions (if the wtd is locally Poissonian) should be independently distributed with probability densities:

$$\begin{aligned} P(\delta t_i) &= 2\lambda_i \exp(-2\lambda_i \delta t_i) \\ P(\delta \tau_i) &= \lambda_i \exp(-\lambda_i \delta \tau_i) \end{aligned}$$

Now a stochastic variable, H , is introduced:

$$H = \frac{\delta t_i}{\delta t_i + \frac{1}{2}\delta \tau_i} \quad (7)$$

such that if the process is locally Poissonian then the cumulative distribution of H will be a uniform distribution between 0 and 1:

$$F(H) = \int_0^\infty 2\lambda e^{-2\lambda x} \int_0^{2x[(1/H)-1]} \lambda e^{-\lambda y} dy dx = 1 - H \quad (8)$$

[39] Figure 6 shows the plots of observed H (sorted) against the theoretical uniform distribution following from a Poisson assumption for SEPES for the complete time period and active years for the each event list.

[40] Values of H above 0.5 indicate a clustering of events as the $\delta \tau_i$ values are typically lower than twice the δt_i values while voids are indicated by values of H below 0.5. We expect for a process which is locally Poissonian that there will be some clustering and some voids. However, deviation below (above) the straight line indicates a higher than expected number of clusters (voids) meaning that the waiting times are not locally Poissonian.

[41] It is clear from visual inspection that there is a high level of clustering of events with some voids for both the JPL and PSYCHIC events while consecutive NOAA events appear to have approximately the level of voids and clusters

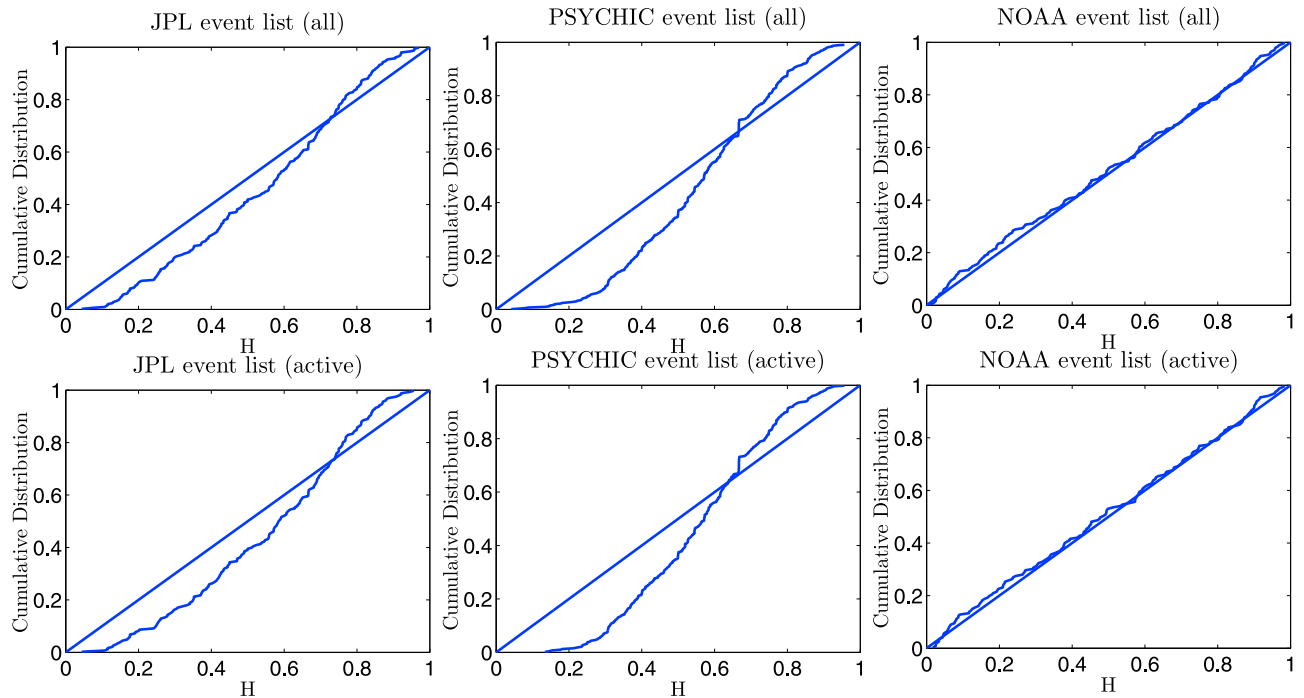


Figure 6. The cumulative distribution function of H for the local Poisson distribution (straight line) and the empirical (observed) cumulative distribution function for H .

expected for a local Poisson distribution. This conclusion is reinforced by the D statistics in a two side Kolmogorov-Smirnov test which are shown in Table 4 which shows that the null hypothesis of a local Poisson can be rejected at the 99% level in all cases other than the NOAA list. There is no significant change to the results with the inclusion or exclusion of the solar quiet years.

[42] The deviation from a local Poisson distribution in the cases of the JPL and PSYCHIC event lists indicates that consecutive events are not independent, that there is a level of memory at work in the system and therefore that the events are not truly random. The test for local Poisson distribution shows no indication of a short-term time dependence (from event to event) for waiting times for the NOAA event list (required for the Poisson process and time-dependent Poisson process) but this does not take into account a longer-term time dependence. When using the NOAA event list it was shown in section 3.2 that the process was not stationary and in section 3.3 that the event rate does not follow a Poisson distribution.

3.5. Lévy Process

[43] It has been found that the process cannot be considered stationary and in both the JPL and the PSYCHIC cases there is strong evidence of local event interdependence. We now investigate a distribution that allows for these factors, the Lévy distribution.

[44] The Lévy skew alpha stable distribution has four free parameters, for parsimony we exclude the skewness and shift parameters which leaves us with the symmetric, centered Lévy process. This distribution is related to the Gaussian but it has a fatter tail determined by a characteristic exponent, μ , and was first suggested to model SEP event waiting times by *Gabriel and Patrick* [2003]. The

transform of the symmetric Lévy distribution into the time domain has two free parameters and is given by

$$P(\Delta t) = \exp(-|c\Delta t|^\mu) \quad (9)$$

[45] This is sometimes called the characteristic function of the symmetric Lévy distribution. The exponent, μ , must lie in the range $[0, 2]$, for a value of $\mu = 2$ the Gaussian distribution is recovered and if the $\mu = 1$ the Cauchy distribution is recovered [Nolan, 2009]. The c parameter is the scaling parameter.

[46] The pdf of the Lévy distribution is given by

$$P(k) = \frac{1}{\pi} \int_0^\infty \exp(-|c\Delta t|^\mu) \cos(k\Delta t) d\Delta t \quad (10)$$

which is the inverse Fourier transform of equation (9) where $P(k)$ is probability of seeing k events in 1 day. This cannot be evaluated analytically but there are methods for numerically evaluating the integral [see *Weron*, 1996, and references therein].

[47] It has been suggested that the integral distributions of both SEP event fluence and waiting times can be fit by power functions and exhibit “fractal” or “scale invariant” behavior leading to parallels between the size of SPEs and earthquakes modeled by the Gutenberg-Richter distribution and the possibility that SPEs are a self-organized critical

Table 4. Significance Level for Rejection of the Independence or Poissonian Nature of Consecutive Events

Significance Level (%)	Complete Time Period	Active Years
JPL	99.975	99.994
PSYCHIC	>99.999	>99.999
NOAA	28.620	4.143

(SOC) phenomenon [Xapsos *et al.*, 2006; Gabriel and Patrick, 2003]. The presence of a characteristic scale in, for example, the exponential distribution destroys the continuous-scale invariance property [Laherrère and Sornette, 1998].

[48] The stretched exponential function similar in form to equation (9) was introduced by Laherrère and Sornette [1998] as an alternative to the power law for “fat tail” distributions seen in nature and economics where there appeared to be natural curvature on double logarithmic axis plots deviating from the straight line predicted by power laws. This deviation was additional to the existing limitation resulting from a finite critical system (such as a limited Earth for the production of earthquakes) where a power law must give way to another regime with exponential decay.

[49] This scale invariant property combined with and indication of memory in the system led Lepreti *et al.* [2001] to fit the waiting times of solar flares numerically with a Lévy pdf (equation (10)). The pdf results in a power law at high waiting times given by

$$P(\Delta t) \sim \Delta t^{-(1+\mu)} \quad (11)$$

[50] However, the data indicates a deviation from a power law at both extremes and therefore here we fit the characteristic function.

4. Results

4.1. Event Waiting Times

[51] Having established three possible functions for the waiting time distributions (equations (2), (6) and (9)) we now interpret each of the distribution parameters, λ , q , c and μ as free parameters and fit them to the waiting time data from each event list (JPL, PSYCHIC and NOAA). We consider the waiting time to be from the onset of one event to the onset of the next which covers the complete time line and the Fourier transform of the function would therefore yield the event frequency.

4.1.1. Distribution Fits

[52] To fit the waiting times the values for each bin (Y_i) were calculated by first dividing the number of waiting times in each bin by the total number of waiting times considered and then normalized by dividing by the bin width. As a result the area of the histogram of the Y vector will be equal to 1 which is a necessity for any pdf. The bins were chosen to be uniformly distributed on a logarithmic axis and therefore the higher–waiting time bins are far larger than the lower waiting times which is favorable due to the sparsity of higher waiting times.

[53] The functions applicable in the time domain for each of the distributions introduced in section 3 were fitted to the binned data for each of the event lists introduced in section 2. We have performed these fits by first minimizing the sum of the squared residuals of the natural logarithms of Y_i , $S^2 = \sum_{i=1}^n (\ln(Y_i) - \ln(P(\Delta t)_i))^2$, by applying a iterative nonlinear least squared method using Gaussian elimination and then minimizing the χ^2 values in the natural domain ($\chi^2 = \sum_{i=1}^n \frac{(Y_i - P(\Delta t)_i)^2}{P(\Delta t)_i}$). The square root of the product of the two fitting parameters, $\sqrt{S^2 \chi^2}$, was then minimized using an iterative procedure. The reason for this choice of

a combination of fitting parameters was that it was found that the χ^2 fit was heavily weighted to the low waiting times (durations), to the extent that the contribution of the majority of points was negligible, while the S^2 values were more evenly weighted. However, as there is greater uncertainty at high–waiting time (duration) points due to the smaller number of events in each bin, fitting to these values is less important so to reflect this it was decided to combine the two fitting methods. This is a nonstandard method, however, there is good reason behind the choice and the S^2 values (of the natural logarithms) and the χ^2 values (in the natural domain) are both included in Appendix A.

[54] To clarify our decision in choosing the $\sqrt{S^2 \chi^2}$ goodness-of-fit criterion we investigate the two instances where the results in Table 6 differ for one or other of the individual fitting parameters, S^2 and χ^2 .

[55] 1. In the PSYCHIC event list (active years), the χ^2 goodness-of-fit parameter indicates the Lévy distribution is a better fit than the Poisson distribution. This difference in the χ^2 values is $\sim 2\%$. Studying the data we find that the Poisson distribution is a better fit to 5 out of the 9 data points than the Lévy distribution. In this case the Lévy distribution is a better fit to 3 binned data points with 1 data point approximately equidistant. However, as the 3 data points the Lévy distribution is a better fit to are at the lower end of the distribution the χ^2 value is lower overall (see Table A11). This shows the excessive bias given to the lower–waiting time points by a χ^2 fit and justifies combining it with the S^2 goodness-of-fit parameter. (There is a general trend that the Poisson distribution is poorly fit to data at the lowest waiting times; this is likely to result from a failure to allow for the clustering of SEPEs highlighted in sections 3.2 and 3.4.)

[56] 2. In the NOAA event list (active years), the S^2 goodness-of-fit parameter indicates the Lévy distribution is worse than the time-dependent Poisson distribution (see Table A9). In this case both distributions are very well fitted to the data but with the Lévy a better fit over the first 10 points (see Figure 9 (bottom)). However, the majority of contribution for the S^2 comes from the last data point (the longest waiting time) so the total S^2 goodness of fit indicates that the time-dependent Poisson distribution is the best fit to the data. The final bin contained only 2 events, so the confidence in it is low but it was able to significantly alter the result; this example justifies not using the S^2 parameter alone.

[57] 3. The product of the goodness-of-fit parameters was taken rather than the sum as in some cases one parameter was significantly larger than the other making the smaller contribution negligible. The square root was taken to counter any exaggeration of differences between distributions caused by multiplying the two goodness-of-fit parameters.

[58] Using a goodness-of-fit criterion of simply $S^2 \times \chi^2$ served to exaggerate any differences while the $\sqrt{S^2 \chi^2}$ criterion gave a more balanced measure of the goodness of fit.

[59] At all stages we have attempted to ensure there was no bias and that the results were not dependent upon the binning. To do this, the bins were varied and the quality of fit values displayed are the mean values across the 5 bins used for each event list.

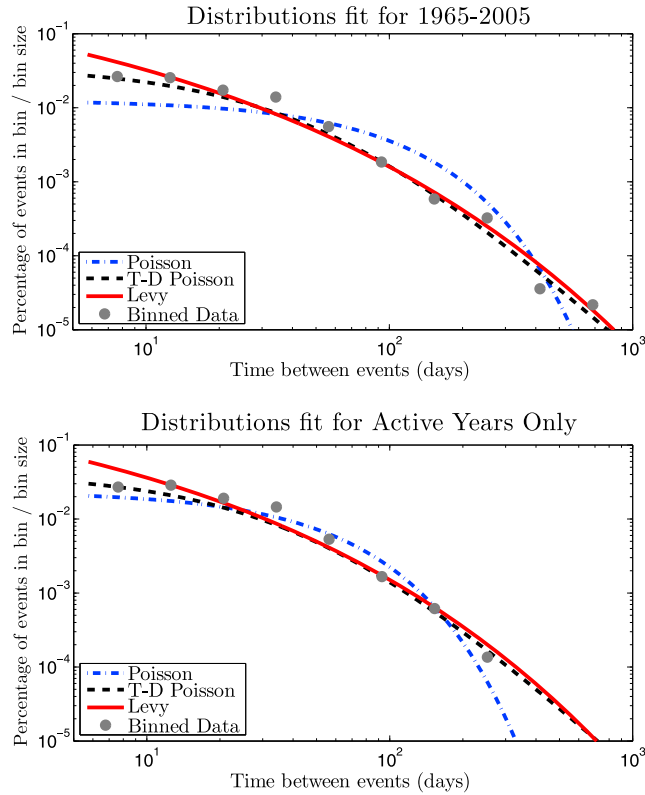


Figure 7. Waiting times and distributions for JPL events for (top) complete time period and (bottom) active years only.

4.1.2. Quality of Fits

[60] The distribution parameters for each of the fits are given in Table 5. The fits for the stated parameters for the JPL, PSYCHIC and NOAA event waiting times for both the complete time periods and the active years only are shown in Figures 7, 8, and 9, respectively. Table 5 and Figures 7, 8, and 9 are just one of 5 binnings that were tested, that with the median bin width. It can be seen that in all but one instance the time-dependent Poisson process and the Lévy process provide superior fits to the Poisson process.

[61] Table 6 shows the quality of fits using the combined fitting parameter, $\sqrt{S^2\chi^2}$, averaged over all 5 binnings used to remove any possible bias. These results show that the time-dependent Poisson process is the best fit for the JPL event list, the Poisson is best for the PSYCHIC (active years only) and the Lévy is best for the PSYCHIC (complete time period) and the NOAA event list. Furthermore, where the Lévy process is not the best it is always a close second whereas in the other two distributions are never both well fit.

[62] The Poisson distribution is clearly the worst fit in 5 out of 6 cases with the exception being the PSYCHIC active year fit (Figure 8, bottom). Differences in the selection of the best fitted distribution could be a result of inherent differences in the event lists or limited data resulting in noise in the system (a possible example of significant noise can be seen in the JPL fit Figure 7 (top)). What is clear is that of the 3 distributions the Lévy is the most robust and does not require that the process is stationary or that events are independent in time. However,

the analysis cannot always unambiguously determine the best fit distribution.

[63] The individual values for constants using each binning used including those for Figures 7, 8, and 9 are listed in Appendix A along with the bin boundaries. Also included in Appendix A are the S^2 , χ^2 and $\sqrt{S^2\chi^2}$ values for all of the fits.

4.1.3. Variation for Different Bins

[64] In addition to mitigating for bias we can use the various binnings to find the variability in the constants. For each event list the lower boundary of the first bin remained constant and the natural logarithm of the bin width was varied which necessarily changed the final bin boundary.

[65] Table 7 shows the variability of the constants using 5 different binnings by taking the range of values divided by the mean value. These constants are displayed for each of the data sets for both the complete time periods and active years only. Table 7 shows that there is some significant variability. The constant which changes the least with the changing binning is the Lévy exponent, μ (mean of 5.10%), while the Lévy scale constant, c (26.87%), shows the most variability. The time-dependent Poisson constant, d (12.93%), appears less variable than the Poisson constant, λ (17.63%). A main cause of variation is a lack of knowledge as to where the final bin boundary should lie and as there are relatively few bins (to maximize the confidence in each point) this can change the results markedly. The bin limits can be found in Appendix A.

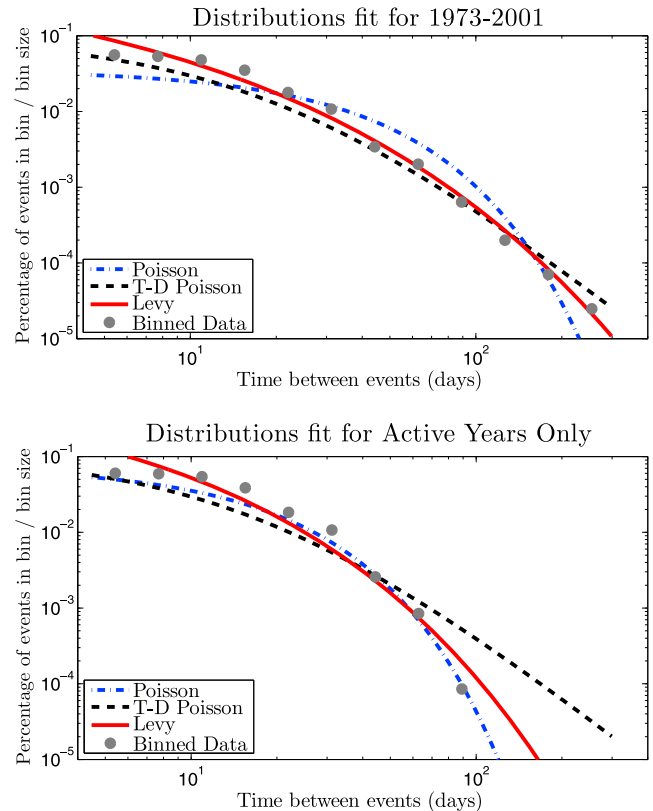


Figure 8. Waiting times and distributions for PSYCHIC events for (top) complete time period and (bottom) active years only.

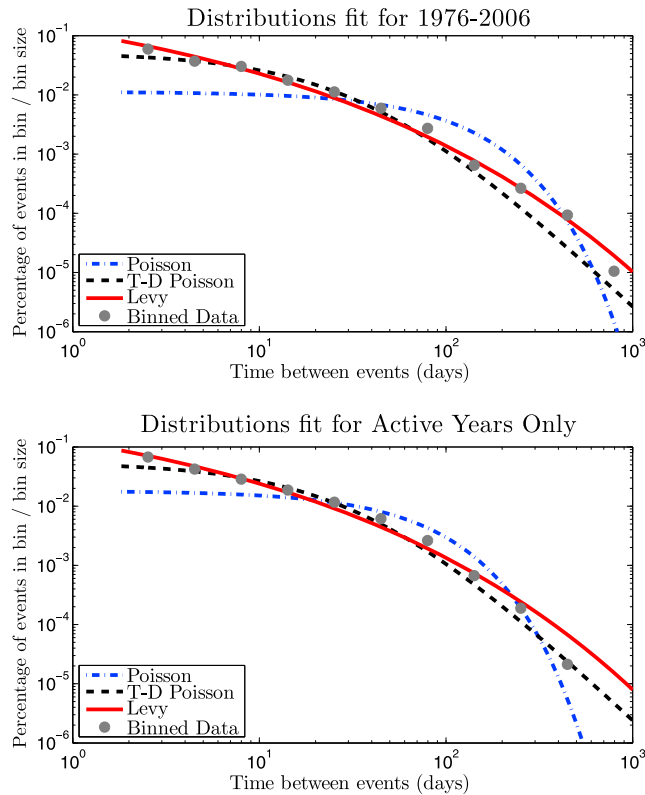


Figure 9. Waiting times and distributions for NOAA events for (top) complete time period and (bottom) active years only.

4.2. Event Durations

[66] Having considered the distribution of the waiting times of events it seems natural to consider the distribution of the durations of the events and see if similar functions may be fit to the data. *Jun et al.* [2007] made a fit of the event durations in their data set to an exponential distribution (the function fit to represent the Poisson process for waiting times), we extend this to the time domain functions derived from the time-dependent Poisson process and the Lévy process. In the case of duration analysis the Δt that previously represented the event waiting times in the equations in section 3 will represent the event durations.

4.2.1. Distribution Fits

[67] The Y_i values for the PSYCHIC events were again determined using exponential bins, on this occasion all 482 event durations were included. As the JPL event list includes only durations of integer days we set the bin boundaries to 0.5 days to avoid bias between bins. Once

Table 5. Constants for Waiting Time Distributions Using Median Binning Width

	JPL	PSYCHIC	NOAA	Years
λ	0.0126	0.0355	0.0113	1976–2006
	0.0235	0.0745	0.0181	active years
ρ	0.0183	0.0489	0.0259	1976–2006
	0.0212	0.0558	0.0273	active years
c	9.0910	1.9230	24.7907	1976–2006
	6.1098	0.9258	19.7865	active years
μ	0.2734	0.3835	0.2412	1976–2006
	0.2917	0.4860	0.2489	active years

Table 6. Quality of SPE Waiting Time Fits as Measured by $\sqrt{S^2\chi^2}$

Event List	Years	Poisson	Time-Dependent Poisson	Lévy
JPL	1976–2006	0.7704	0.0812	0.1089
	active years	0.1764	0.0832	0.0997
PSYCHIC	1976–2006	0.9014	0.3399	0.1378
	active years	0.2099	0.6623	0.2711
NOAA	1976–2006	2.1183	0.1460	0.0562
	active years	0.8224	0.0963	0.0591

again we require larger bins for higher durations where there are fewer events and therefore all the bin limits for the JPL events were set “manually.”

[68] Figure 10 shows the distributions fits for the JPL event list. Figure 11 shows the distributions for the PSYCHIC events and here we have also included a lognormal distribution,

$$P(\Delta t) = \frac{1}{\Delta t \sigma \sqrt{2\pi}} \exp\left(-\frac{(\ln(\Delta t) - \mu)^2}{2\sigma^2}\right) \quad (12)$$

as it seemed appropriate given the low number of short-duration events. Table 8 shows the fitted constants for each distribution for event durations for both lists. Presently data is not available for the durations on the NOAA event list.

4.2.2. Quality of Fits

[69] The fits for the JPL event list are all reasonably good with the Poisson process giving the best results. This supports the result of *Jun et al.* [2007] regarding this distribution while also indicating the possibility of using either of the other two functions for fitting event durations. The main difference between the three fits is at low durations.

[70] When we investigate the PSYCHIC results we find a severe dropoff at low durations. Noting that the lognormal distribution has been used previously to approximate the event fluence [*King*, 1974; *Feynman et al.*, 1990, 1993] we found that the lognormal distribution offered greatly improved results. These two event lists seem to offer very different conclusions for how the event durations are distributed. The $\sqrt{S^2\chi^2}$ for both event lists can be found in Table 9.

4.2.3. Fits Excluding Lowest Durations

[71] As a result of the reduced number of low-duration events seen we also fit the portion of PSYCHIC events with duration above 4.48 days, the lower boundary of the exponential bin which had the highest Y_i previously. Figure 12 includes the original lognormal distribution as well as the Lévy and a version of the Poisson fit to the values above 4.48 days. For the Poisson fit we allowed the λ

Table 7. Range of Constants Expressed as a Percentage of the Mean

	JPL	PSYCHIC	NOAA	Years
λ	13.31	11.49	35.90	1976–2006
	13.00	7.85	24.22	active years
ρ	9.80	6.77	19.01	1976–2006
	13.36	9.97	18.67	active years
c	10.28	8.18	27.20	1976–2006
	52.75	16.21	46.57	active years
μ	1.97	2.08	4.06	1976–2006
	8.80	5.93	7.78	active years

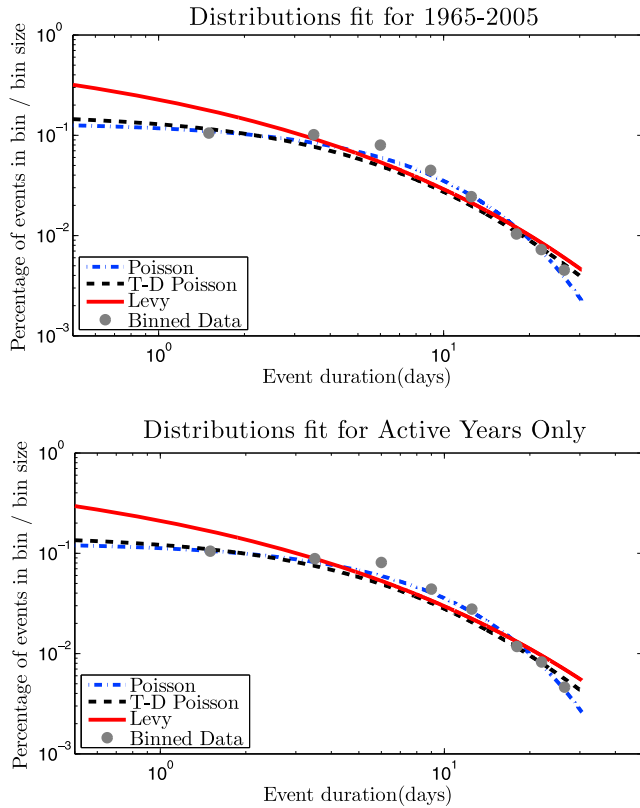


Figure 10. Durations and distributions for JPL events for (top) complete time period and (bottom) active years only.

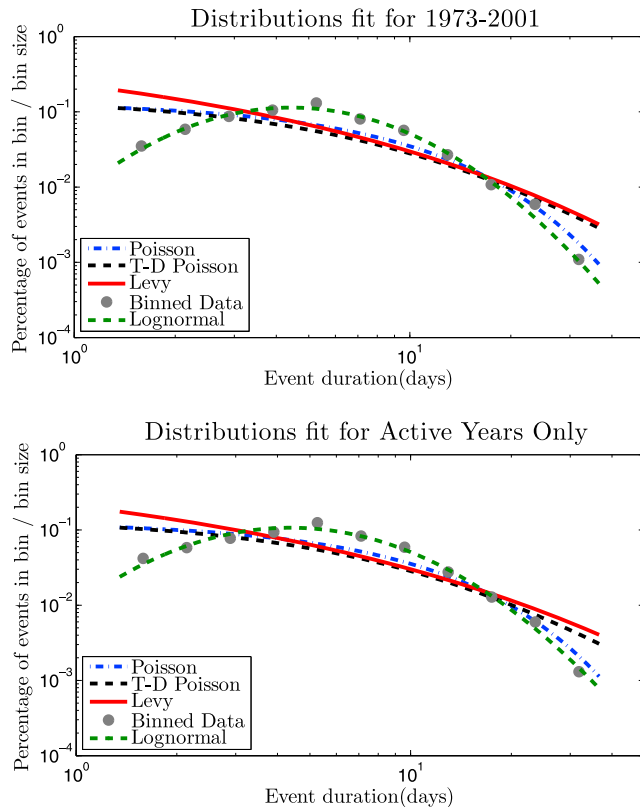


Figure 11. Durations and distributions for PSYCHIC events for (top) complete time period and (bottom) active years only.

Table 8. Constants for Duration Distributions Using Median Binning Width

	JPL	PSYCHIC 1	PSYCHIC 2	Years
λ	0.1342	0.1358	0.1743	1976–2006
	0.1277	0.1295	0.1683	active years
ρ	0.0816	0.0749	-	1976–2006
	0.0754	0.0705	-	active years
c	2.8609	2.7480	0.5213	1976–2006
	3.5023	3.6388	0.5309	active years
μ	0.3770	0.3793	0.6742	1976–2006
	0.3537	0.3488	0.6614	active years
M	-	1.9023	1.9023	1976–2006
	-	1.9347	1.9347	active years
σ	-	0.6440	0.6440	1976–2006
	-	0.6777	0.6777	active years

outside the exponential to vary from the value of that inside the exponential (see equation (2)). This increases the number of fitting parameters by 1 so the number of degrees of freedom is now the same as the Lévy functional fit. The reason for this is that in the exponential domain (or on semilogarithmic axes) the function is a straight line with a fixed intercept but as we have artificially removed all low-duration events the values of the higher durations would not fit to the correct exponential fit. If there were the expected number of low-duration events then the values for the other bins would be reduced allowing a correct fit. It also follows that the Lévy function in this case is also not a real pdf. This is apparent when we compare the area under the Poisson and Lévy fits to that under the lognormal distribution.

[72] In spite of inherent limitations of excluding the lower bins these plots do show that the functions can be fit to the waiting times and JPL event durations can be fit to the higher durations for the PSYCHIC event list although the exclusion of the lower bins which contained 121 events results in the use of only 74.9% of the available data.

5. Discussion

[73] The discussion follows the results for both waiting times and event durations for each data set separately with reasons for any similarities and differences discussed in the conclusion.

5.1. JPL Event List

[74] The waiting time results for the JPL list indicate that the time-dependent Poisson process is the best fit, closely followed by a Lévy process and then a Poisson process. This conclusion is supported by the test for stationarity which concluded that even excluding the solar quiet years the process could not be considered stationary. It was also found that despite attempts to ensure that events were independent (particularly the requirement of a 2 day lag time between events) the likelihood of a future event was affected by the occurrence of a preceding event.

[75] Due to the variable duration of events, as we look at lower waiting times so the number of events for which the

Table 9. Quality of SPE Duration Fits as Measured by $\sqrt{S^2\chi^2}$

Event List	Years	Time-Dependent			
		Poisson	Poisson	Lévy	Lognormal
JPL	1976–2006	0.0452	0.1322	0.1788	-
	active years	0.0343	0.1241	0.1734	-
PSYCHIC	1976–2006	0.6854	1.1210	1.3960	0.0405
	active years	0.5733	0.9664	1.2514	0.0408

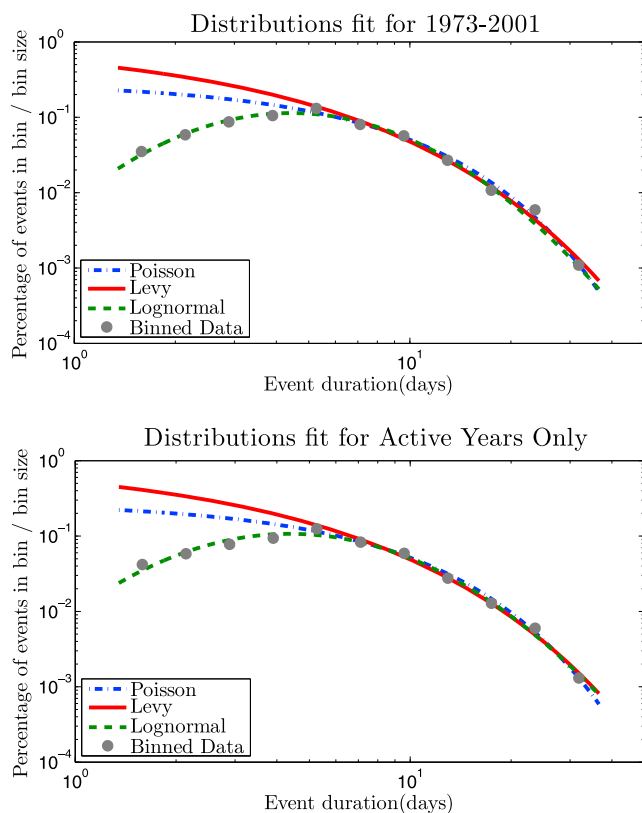


Figure 12. Durations and distributions for PSYCHIC events for (top) complete time period and (bottom) active years only.

waiting time is possible is reduced. This “non-point-like nature” of SEPES gives a possible reason for the time-dependent Poisson process being better fit to the waiting time data than the Lévy process. The effect of this lower limit resulting from the previous event duration is reflected in the data set as there is only 1 event with a waiting time below the lowest bin limit of 5.8 days (see Table 10). This reduction is an unavoidable artifact of the data set using this event definition.

[76] To allow for comparison with the waiting times plot produced by *Feynman et al.* [2002] we have produced a plot with axes with a logarithmic ordinate but a linear abscissa (Figure 13). It can be seen that although there is significant scatter, the Lévy and time-dependent Poisson fits are better than the straight line Poisson fit.

[77] The durations of the SEPES from the JPL list are best fit by a Poisson process (exponential distribution). It is possible that there are a reduced number of short-

Table 10. Percentage of Events Used for Each Event List

	Total Events	Events Used	Percent of Events Used	Years
JPL	275	274	99.64	1976–2006
	243	242	99.59	active years
PSYCHIC	481	457	95.01	1976–2006
	404	383	94.80	active years
NOAA	224	214	95.54	1976–2006
	201	191	95.02	active years

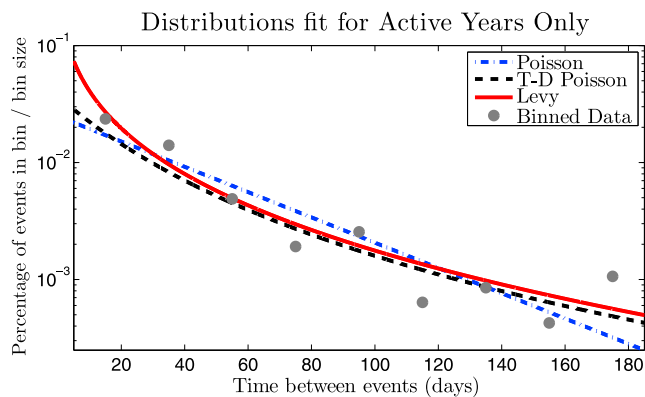


Figure 13. JPL waiting time plot with axes with a logarithmic ordinate but a linear abscissa.

duration events due to the 10^6 cm^{-2} lower fluence limit. A breakdown of the lowest event durations shows that out of 276 events there are 29 occurrences of both 1 and 2 day event durations and 33 occurrences of 3 day event durations before a steady decline. The detection of smaller events is often difficult and may be dependent on other activity at the time so it is likely that this is unavoidable. To test the results of event duration on this event definition it would be desirable to reduce the sampling time so that fractions of days were possible.

5.2. PSYCHIC Event List

[78] The PSYCHIC list was best fit by the Lévy process for the complete time period but better fit by the Poisson process when considering only the active years. This is surprising as it was found that during active years that process was not stationary and it showed the greatest deviation from a local Poisson assumption. To be better fit by the Lévy process we would expect a greater number of shorter waiting time events and fewer waiting times of between ~ 15 and 40 days. The effect of the non-point-like nature of events could be more strongly felt here than for the JPL list. The ratio between the mean waiting time and mean duration (shown by Table 11) is only 1.89 for the PSYCHIC list active years. If events are sparse then the effect of the duration will be less strongly felt whereas if they are many the effect will be stronger. The longer the event durations in comparison to the waiting times the greater the dropoff at low waiting times.

[79] The duration fits for the PSYCHIC list show a reducing number of the lowest event durations not predicted by any of the fitted distributions resulting in a better fit for the complete data set by a lognormal distribution. The peak of event duration is between 5 and 6 days with 56 out of the

Table 11. Mean Values of Waiting Times and Durations and the Ratios Between Them

	Years	Waiting Time (days)	Duration (days)	Ratio
JPL	1965–2005	53.84	7.08	7.60
	active years	35.50	6.48	5.48
PSYCHIC	1973–2007	21.24	8.22	2.58
	active years	13.47	7.13	1.89
NOAA	1976–2006	49.93	-	-
	active years	32.10	-	-

482 durations (11.6%) falling between these limits. It should be noted that while inspiration for using the lognormal distribution fit was taken from the JPL model [Feynman *et al.*, 1993], even in the case of event fluences considered by that model there was an ever increasing number of lower-fluence events not predicted by the distribution.

[80] It is possible that as longer-duration events are caused by wider, more energetic CMEs [Wang and Wang, 2004] they have an increased chance of being observed at Earth and that this could contribute to a reduction in the number of low-duration events seen. However, it is likely that the biggest contributing factors to this reduction are: an inability to detect the smaller events (which are typically shorter in duration) above the background level and the requirement of minimum peak flux values for events to remain in the PSYCHIC list which would exclude many more shorter-duration events than longer ones similar to the fluence cutoff used in the JPL list.

5.3. NOAA Event List

[81] The NOAA event list was the only one of the three where events were not found to be locally dependent upon one another. However, there were still longer-term dependencies as a hypothesis for stationarity could be rejected at the 95% confidence level in both the complete time period and when considering the active years only. The result of the waiting time fits was more comprehensively opposed to a conclusion that the process was Poissonian while the Lévy process was the best fit. The lowest bin limit of only 1.8 days indicates that the effect of the events being non-point-like was less prominent here. We can hypothesize that the reason for this are the higher thresholds used in the event definition resulting in events being shorter while being comparable in number to the JPL list. Unfortunately data on the event durations to quantitatively validate this conclusion were not available.

6. Summary and Conclusions

[82] It is known that there was variation between the rate of SEPES during solar maximum and solar minimum [Feynman *et al.*, 1990]. It had been assumed that, by using event definitions which linked all related events, during solar maximum the process could be considered Poissonian as the mean SEP event rate was steady. We have reexamined the time distribution of SEPES, tested the Poissonian requirements and proposed two new possible distributions: a time-dependent Poisson process and a Lévy process.

[83] The tests for stationarity show that regardless of event definition the process cannot be considered stationary even considering only active periods of the solar cycle as we are able to reject the null hypothesis of stationarity at the 95% confidence level in all cases. The tests for local independence of events (at the 99% confidence level) show memory in the system for both the JPL and PSYCHIC event lists but that by setting thresholds to exclude smaller events we can create a list where consecutive events are not locally dependent upon one another (e.g., the NOAA list). However, even in this case there remains a longer-term time dependence of event frequency as shown by the test for stationarity. We find that in 2 out of the 3 cases (JPL and

NOAA) the Poisson function is poorly fit to the waiting time data in comparison with the Lévy fit confirming the earlier results of stationarity. In the 1 case where the Poisson function was better fit (PSYCHIC) the process was neither stationary nor were events locally independent. We must therefore conclude that the waiting time distribution has been skewed by another factor and the most likely candidate appears to be the significance of the event durations which results in a reduced number of the lowest waiting times and an increase in the number of longer waiting times. This makes the distribution of waiting times appear more Poissonian when in fact all other evidence points to a non-Poissonian distribution of events in time.

[84] The time-dependent Poisson process was previously applied to solar flares and CMEs by Wheatland [2000, 2003]. The time-dependent Poisson was best fit to the waiting times of the JPL event list. With regards to solar flares Lepreti *et al.* [2001] noted that since this distribution reduces to a power law for high waiting times the result was at least qualitatively correct despite being based upon incorrect assumptions. We might draw a similar conclusion from our results as, despite event interdependence, the distribution gives good results with only one free parameter in all but 1 instance. However, in the case of the active years for PSYCHIC event list the time-dependent Poisson process did not fit the data well which was to be expected given the poor fit of the exponential distribution to the event rate (see Figure 5).

[85] The Lévy process was the best fit in the case of the NOAA event list and well fit in all other cases with a comparable goodness-of-fit parameter to the best fitting function (see Table 6). This process allows for an interdependence of events suggested by the results of tests for local independence and stationarity. Initially suggested to fit to SEPE waiting times by Gabriel and Patrick [2003] the Lévy process offers the most robust solution to the problem of waiting time fits. The trade-off is that the Lévy process has two free parameters rather than one; this is statistically undesirable as we desire parsimony (preference for the smallest number of free parameters). The resulting Lévy distribution which would apply to event frequency is a heavy tailed distribution meaning that it is skewed predicting a less stable SEP environment characterized by periods of high activity and periods of lower activity as well as the likelihood of future events being influenced by the occurrence of recent events. This agrees with previous analysis by Xapsos *et al.* [2006] and Gabriel and Patrick [2003] where it was concluded that SEPES might be a self-organized critical (SOC) phenomenon and although it is likely that it is impossible to predict the occurrence of events there is a long-term correlation between SEPES similar to other natural phenomena such as earthquakes. It appears that deviation from the Lévy waiting time fit can be attributed to the non-point-like nature of SEPES.

[86] We have shown using the JPL and PSYCHIC event lists that it is possible that the waiting time between SEPES and the durations of these events may be fitted with functions from the same family of distributions. However, as with the event waiting times the number of events with the shortest durations is lower than that predicted by the Poisson, time-dependent Poisson and Lévy distributions.

This reduction is possibly contributed to by the increased likelihood of a larger event being observed compared to a smaller one due to the width of the CME. However, more significant factors are the exclusion of and inability to detect the smallest events resulting in a reduced number of low-duration events in the lists. As a result we found that for the PSYCHIC list a lognormal distribution was the best fit to the data; this distribution has been previously applied to SEP event fluences [Feynman *et al.*, 1993].

[87] There is evidence that if an event (of whatever size) has just occurred that there is increased likelihood of another occurring. The difference in result for the NOAA event list (where we have higher-flux thresholds) for event independence might indicate that we get clustering of smaller, lower peak flux, events (excluded in the NOAA list) around the larger, higher peak flux, events much like we might expect preshocks and aftershocks either side of a large earthquake. This is consistent with the idea that SEPEs, like earthquakes, are an SOC phenomenon.

Appendix A: Supporting Material

[88] Tables A1–A17 provide a complete catalog of parameter input and output at all stages of the work.

Table A1. Constants for Distributions for JPL Event List

	Binning 1	Binning 2	Binning 3	Binning 4	Binning 5	Years
λ	0.0127	0.0111	0.0126	0.0111	0.0126	1976–2006
	0.0227	0.0207	0.0235	0.0210	0.0236	active years
ρ	0.0182	0.0189	0.0183	0.0191	0.0173	1976–2006
	0.0217	0.0218	0.0212	0.0211	0.0190	active years
c	9.0597	8.4971	9.0910	8.1884	9.0542	1976–2006
	5.8589	5.7124	6.1098	5.6672	9.0896	active years
μ	0.2728	0.2766	0.2734	0.2782	0.2730	1976–2006
	0.2938	0.2965	0.2917	0.2960	0.2710	active years

Table A2. Constants for Distributions for PSYCHIC Event List

	Binning 1	Binning 2	Binning 3	Binning 4	Binning 5	Years
λ	0.0355	0.0350	0.0355	0.0360	0.0320	1976–2006
	0.0776	0.0718	0.0745	0.0724	0.0731	active years
ρ	0.0494	0.0488	0.0489	0.0467	0.0500	1976–2006
	0.0542	0.0577	0.0558	0.0522	0.0558	active years
c	1.9360	2.0139	1.9230	2.0863	2.0212	1976–2006
	1.0288	0.9563	0.9258	1.0855	0.9294	active years
μ	0.3832	0.3796	0.3835	0.3756	0.3791	1976–2006
	0.4687	0.4809	0.4860	0.4578	0.4850	active years

Table A3. Constants for Distributions for NOAA Event List

	Binning 1	Binning 2	Binning 3	Binning 4	Binning 5	Years
λ	0.0114	0.0134	0.0113	0.0093	0.0117	1976–2006
	0.0231	0.0206	0.0181	0.0213	0.0201	active years
ρ	0.0222	0.0271	0.0259	0.0269	0.0268	1976–2006
	0.0251	0.0256	0.0273	0.0258	0.0301	active years
c	24.2685	31.4232	24.7907	24.1726	28.6271	1976–2006
	22.9500	20.3264	19.7865	21.2535	30.4789	active years
μ	0.2423	0.2326	0.2412	0.2418	0.2359	1976–2006
	0.2424	0.2484	0.2489	0.2455	0.2300	active years

Table A4. $\sqrt{S^2\chi^2}$ Values for JPL Fits

Binning	Years	Poisson	Time-Dependent	
			Poisson	Lévy
1	1965–2005	0.7979	0.0796	0.0785
	active years	0.1883	0.0830	0.0828
2	1965–2005	0.9427	0.0833	0.1185
	active years	0.2232	0.0803	0.1047
3	1965–2005	0.7119	0.0811	0.1143
	active years	0.1365	0.0789	0.1030
4	1965–2005	0.8606	0.0923	0.1352
	active years	0.1868	0.0835	0.1086
5	1965–2005	0.5390	0.0696	0.0983
	active years	0.1471	0.0903	0.0992
Mean	1965–2005	0.7704	0.0812	0.1089
	active years	0.1764	0.0832	0.0997

Table A5. $\sqrt{S^2\chi^2}$ Values for PSYCHIC Fits

Binning	Years	Poisson	Time-Dependent	
			Poisson	Lévy
1	1973–2001	1.0069	0.4177	0.1751
	active years	0.2874	0.7774	0.3576
2	1973–2001	0.9525	0.3514	0.1435
	active years	0.2369	0.7517	0.2899
3	1973–2001	0.7873	0.3156	0.1069
	active years	0.1805	0.6744	0.2697
4	1973–2001	0.7749	0.2739	0.1108
	active years	0.1707	0.4712	0.1744
5	1973–2001	0.9852	0.3407	0.1528
	active years	0.1743	0.6366	0.2641
Mean	1973–2001	0.9014	0.3399	0.1378
	active years	0.2099	0.6623	0.2711

Table A6. $\sqrt{S^2\chi^2}$ Values for NOAA Fits

Binning	Years	Poisson	Time-Dependent	
			Poisson	Lévy
1	1976–2006	2.1594	0.1639	0.0703
	active years	0.7278	0.1133	0.0483
2	1976–2006	1.8107	0.1322	0.0616
	active years	0.8217	0.0788	0.0641
3	1976–2006	2.0426	0.1560	0.0525
	active years	1.0788	0.1049	0.0646
4	1976–2006	2.6603	0.1480	0.0413
	active years	0.7855	0.0968	0.0382
5	1976–2006	1.9182	0.1299	0.0555
	active years	0.6982	0.0879	0.0805
Mean	1976–2006	2.1183	0.1460	0.0562
	active years	0.8224	0.0963	0.0591

Table A7. S^2 Values for JPL Fits

Binning	Years	Poisson	Time-Dependent	
			Poisson	Lévy
1	1965–2005	9.2676	0.8955	0.8733
	active years	1.6267	0.6892	0.6749
2	1965–2005	12.2399	1.1945	1.4457
	active years	2.3514	0.7263	0.8606
3	1965–2005	9.8122	1.0127	1.2653
	active years	1.3758	0.6369	0.8128
4	1965–2005	11.6083	1.3638	1.7035
	active years	1.7932	0.6678	0.8341
5	1965–2005	6.2464	0.6474	0.8910
	active years	1.4818	0.6806	0.7988
Mean	1965–2005	9.8349	1.0228	1.2358
	active years	1.7258	0.6801	0.7962

Table A8. S^2 Values for PSYCHIC Fits

Binning	Years	Time-Dependent		
		Poisson	Poisson	Lévy
1	1973–2001	8.9476	2.7709	1.2257
	active years	1.7468	6.1199	2.9266
2	1973–2001	9.1074	2.4050	1.1216
	active years	1.3928	6.4379	2.0328
3	1973–2001	7.0427	2.0609	0.6385
	active years	0.9177	5.6244	1.7953
4	1973–2001	6.9992	1.6164	0.8015
	active years	0.8253	3.0209	1.0868
5	1973–2001	10.0424	2.5133	1.3057
	active years	0.9023	5.4833	1.8685
Mean	1973–2001	8.4279	2.2733	1.0186
	active years	1.1570	5.3373	1.9420

Table A12. The χ^2 Values for NOAA Fits

Binning	Years	Time-Dependent		
		Poisson	Poisson	Lévy
1	1976–2006	0.3345	0.0141	0.0068
	active years	0.1238	0.0172	0.0042
2	1976–2006	0.2328	0.0043	0.0039
	active years	0.1415	0.0124	0.0043
3	1976–2006	0.3283	0.0077	0.0037
	active years	0.1990	0.0133	0.0025
4	1976–2006	0.3981	0.0048	0.0044
	active years	0.1272	0.0123	0.0030
5	1976–2006	0.2596	0.0044	0.0036
	active years	0.1329	0.0063	0.0014
Mean	1976–2006	0.3107	0.0071	0.0045
	active years	0.1449	0.0123	0.0031

Table A9. S^2 Values for NOAA Fits

Binning	Years	Time-Dependent		
		Poisson	Poisson	Lévy
1	1976–2006	13.9417	1.9097	0.7263
	active years	4.2781	0.7454	0.5538
2	1976–2006	14.0845	4.0392	0.9797
	active years	4.7728	0.5002	0.9545
3	1976–2006	12.7098	3.1435	0.7411
	active years	5.8476	0.8301	1.6854
4	1976–2006	17.7759	4.5374	0.3914
	active years	4.8497	0.7587	0.4805
5	1976–2006	14.1721	3.8050	0.8519
	active years	3.6673	1.2236	4.7372
Mean	1976–2006	14.5368	3.4870	0.7381
	active years	4.6831	0.8116	1.6823

Table A10. The χ^2 Values for JPL Fits

Binning	Years	Time-Dependent		
		Poisson	Poisson	Lévy
1	1965–2005	0.0687	0.0071	0.0071
	active years	0.0218	0.0100	0.0102
2	1965–2005	0.0726	0.0058	0.0097
	active years	0.0212	0.0089	0.0127
3	1965–2005	0.0517	0.0065	0.0103
	active years	0.0135	0.0098	0.0131
4	1965–2005	0.0638	0.0062	0.0107
	active years	0.0194	0.0104	0.0141
5	1965–2005	0.0465	0.0075	0.0108
	active years	0.0146	0.0120	0.0123
Mean	1965–2005	0.0607	0.0066	0.0097
	active years	0.0181	0.0102	0.0125

Table A11. The χ^2 Values for PSYCHIC Fits

Binning	Years	Time-Dependent		
		Poisson	Poisson	Lévy
1	1973–2001	0.1133	0.0630	0.0250
	active years	0.0473	0.0987	0.0437
2	1973–2001	0.0996	0.0514	0.0184
	active years	0.0403	0.0878	0.0413
3	1973–2001	0.0880	0.0483	0.0179
	active years	0.0355	0.0809	0.0405
4	1973–2001	0.0858	0.0464	0.0153
	active years	0.0353	0.0735	0.0280
5	1973–2001	0.0967	0.0462	0.0179
	active years	0.0337	0.0739	0.0373
Mean	1973–2001	0.0967	0.0511	0.0189
	active years	0.0384	0.0830	0.0382

Table A13. Bin End Limits Used for JPL Event List Waiting Time Analysis^a

	Binning 1	Binning 2	Binning 3	Binning 4	Binning 5
Start	5.8	5.8	5.8	5.8	5.8
Bin 1	9.0	9.3	9.5	9.7	10.0
Bin 2	14.2	14.9	15.6	16.4	17.3
Bin 3	22.2	23.9	25.8	27.8	30.0
Bin 4	34.8	38.5	42.5	47.0	51.9
Bin 5	54.6	61.9	70.1	79.4	90.0
Bin 6	85.6	99.5	115.6	134.3	156.0
Bin 7	134.3	160.0	190.6	227.0	270.4
Bin 8	210.6	257.2	314.2	383.8	468.7
Bin 9	330.3	413.6	518.0	648.7	812.4
Bin 10	518.0	665.1	854.1	1096.6	
Bin 11	812.4	1069.6			

^aTime analysis is in days.

Table A14. Bin End Limits Used for PSYCHIC Event List Waiting Time Analysis^a

	Binning 1	Binning 2	Binning 3	Binning 4	Binning 5
Start	4.5	4.5	4.5	4.5	4.5
Bin 1	6.0	6.2	6.4	6.5	6.7
Bin 2	8.2	8.6	9.0	9.5	10.0
Bin 3	11.0	11.9	12.8	13.8	14.9
Bin 4	14.9	16.4	18.2	20.1	22.2
Bin 5	20.1	22.8	25.8	29.2	33.1
Bin 6	27.1	31.5	36.6	42.5	49.4
Bin 7	36.6	43.6	51.9	61.9	73.7
Bin 8	49.4	60.3	73.7	90.0	109.9
Bin 9	66.7	83.5	104.6	131.0	164.0
Bin 10	90.0	115.6	148.4	190.6	244.7
Bin 11	121.5	160.0	210.6	277.3	365.0
Bin 12	164.0	221.4	298.9		
Bin 13	221.4	306.4			
Bin 14	298.9				

^aTime analysis is in days.

Table A15. Bin End Limits Used for NOAA Event List Waiting Time Analysis^a

	Binning 1	Binning 2	Binning 3	Binning 4	Binning 5
Start	1.8	1.8	1.8	1.8	1.8
Bin 1	3.1	3.2	3.2	3.3	3.4
Bin 2	5.2	5.5	5.8	6	6.4
Bin 3	8.8	9.5	10.2	11	11.9
Bin 4	14.9	16.4	18.2	20.1	22.2
Bin 5	25.2	28.5	32.3	36.6	41.5
Bin 6	42.5	49.4	57.4	66.7	77.5
Bin 7	71.9	85.6	102	121.5	144.7
Bin 8	121.5	148.4	181.3	221.4	270.4
Bin 9	205.4	257.2	322.1	403.4	505.2
Bin 10	347.2	445.9	572.5	735.1	943.9
Bin 11	587	772.8	1017.4	1339.4	
Bin 12	992.3				

^aTime analysis is in days.

Table A16. Bins Used for Duration Analysis^a

	JPL	PSYCHIC
Start	0.5	1.35
Bin 1	2.5	1.82
Bin 2	4.5	2.46
Bin 3	7.5	3.32
Bin 4	10.5	4.48
Bin 5	14.5	6.05
Bin 6	21.5	8.17
Bin 7	22.5	11.02
Bin 8	30.5	14.88
Bin 9		20.09
Bin 10		27.11
Bin 11		36.60

^aDuration analysis is in days.

Table A17. JPL Event List

Event Number	Start Date		Duration (days)	Fluence >10 MeV
	Year	Day of Year		
1	1965	37	3	1.60E + 07
2	1965	277	4	2.60E + 06
3	1966	83	4	1.10E + 07
4	1966	124	6	1.50E + 06
5	1966	189	5	6.40E + 07
6	1966	241	27	1.00E + 09
7	1967	12	2	3.60E + 06
8	1967	29	20	1.10E + 09
9	1967	59	9	7.10E + 06
10	1967	71	4	1.60E + 07
11	1967	145	11	7.80E + 08
12	1967	158	13	2.40E + 07
13	1967	304	22	3.00E + 07
14	1967	338	5	2.50E + 07
15	1967	351	7	1.50E + 07
16	1968	162	5	1.90E + 08
17	1968	190	10	4.70E + 07
18	1968	271	12	7.40E + 07
19	1968	304	10	2.10E + 08
20	1968	324	8	1.00E + 09
21	1968	338	11	2.30E + 08
22	1969	57	6	7.60E + 07
23	1969	81	3	7.10E + 06
24	1969	90	13	7.80E + 07
25	1969	103	16	2.20E + 09
26	1969	269	6	1.80E + 07
27	1969	307	9	6.40E + 08

Table A17. (continued)

Event Number	Start Date		Duration (days)	Fluence >10 MeV
	Year	Day of Year		
28	1969	329	10	7.10E + 06
29	1969	353	5	5.20E + 06
30	1970	29	7	2.80E + 07
31	1970	66	6	6.80E + 07
32	1970	83	18	9.40E + 07
33	1970	151	5	1.40E + 07
34	1970	167	5	2.80E + 06
35	1970	189	3	4.10E + 06
36	1970	203	6	3.60E + 07
37	1970	224	15	9.10E + 08
38	1970	310	9	6.60E + 07
39	1970	347	4	4.20E + 06
40	1970	359	8	1.60E + 07
41	1971	25	16	1.50E + 09
42	1971	92	4	3.00E + 06
43	1971	97	5	3.20E + 07
44	1971	111	5	4.30E + 06
45	1971	133	11	1.40E + 07
46	1971	245	17	3.90E + 08
47	1971	278	5	7.00E + 06
48	1972	109	6	3.00E + 07
49	1972	150	9	7.60E + 07
50	1972	161	15	4.00E + 07
51	1972	202	15	5.40E + 07
52	1972	217	23	1.10E + 10
53	1972	304	5	6.00E + 07
54	1973	103	7	8.20E + 06
55	1973	120	11	1.60E + 07
56	1973	211	6	7.20E + 06
57	1973	251	5	1.90E + 07
58	1973	308	3	4.70E + 06
59	1974	160	4	4.40E + 06
60	1974	185	8	2.40E + 08
61	1974	255	25	3.30E + 08
62	1974	310	4	1.30E + 07
63	1975	233	4	6.60E + 06
64	1976	84	9	5.40E + 06
65	1976	122	5	1.00E + 08
66	1976	236	3	1.00E + 07
67	1977	204	9	6.10E + 06
68	1977	252	24	4.30E + 08
69	1977	286	3	3.90E + 06
70	1977	326	7	2.80E + 08
71	1978	3	11	1.20E + 07
72	1978	45	10	1.50E + 09
73	1978	99	8	7.00E + 07
74	1978	108	28	2.40E + 09
75	1978	152	5	1.80E + 07
76	1978	175	7	5.30E + 07
77	1978	194	7	3.20E + 07
78	1978	206	5	2.70E + 06
79	1978	251	3	2.80E + 06
80	1978	267	15	2.90E + 09
81	1978	283	7	8.60E + 06
82	1978	315	5	1.80E + 07
83	1978	347	5	6.20E + 06
84	1979	49	6	1.60E + 07
85	1979	62	16	2.10E + 07
86	1979	94	4	2.10E + 07
87	1979	158	9	2.10E + 08
88	1979	188	6	2.10E + 07
89	1979	214	15	1.20E + 07
90	1979	232	12	6.00E + 08
91	1979	252	25	3.60E + 08
92	1979	321	3	3.20E + 07
93	1980	12	3	2.80E + 06
94	1980	38	4	3.00E + 06
95	1980	92	8	8.70E + 06
96	1980	199	12	1.20E + 08
97	1980	246	6	3.70E + 06
98	1980	290	9	3.00E + 07

Table A17. (continued)

Event Number	Start Date		Duration (days)	Fluence >10 MeV
	Year	Day of Year		
99	1980	321	6	6.30E + 06
100	1980	329	11	1.40E + 07
101	1981	63	6	3.40E + 06
102	1981	90	8	2.80E + 07
103	1981	101	12	8.50E + 07
104	1981	115	30	1.00E + 09
105	1981	202	7	8.10E + 07
106	1981	221	5	1.40E + 07
107	1981	251	4	7.30E + 06
108	1981	263	9	1.50E + 07
109	1981	282	18	2.10E + 09
110	1981	315	6	5.60E + 06
111	1981	327	4	3.80E + 06
112	1981	340	9	7.70E + 07
113	1981	362	4	7.50E + 06
114	1982	31	13	1.10E + 09
115	1982	66	4	1.10E + 07
116	1982	156	17	7.00E + 07
117	1982	191	12	8.40E + 08
118	1982	204	5	1.20E + 08
119	1982	248	5	1.40E + 07
120	1982	298	3	3.30E + 07
121	1982	326	13	2.50E + 08
122	1982	339	10	5.70E + 08
123	1982	349	9	1.30E + 08
124	1982	360	7	2.10E + 08
125	1983	35	5	1.00E + 08
126	1983	167	13	2.10E + 07
127	1984	32	2	2.40E + 06
128	1984	47	13	1.60E + 08
129	1984	72	9	2.90E + 07
130	1984	116	13	1.30E + 09
131	1985	22	4	8.70E + 06
132	1985	115	7	2.80E + 08
133	1985	193	8	2.30E + 07
134	1986	37	3	7.80E + 07
135	1986	45	4	9.60E + 07
136	1986	65	1	2.00E + 06
137	1986	124	1	3.00E + 06
138	1987	312	2	3.00E + 07
139	1987	364	8	9.50E + 07
140	1988	85	2	5.00E + 06
141	1988	182	1	3.00E + 06
142	1988	238	6	1.40E + 07
143	1988	279	1	1.00E + 06
144	1988	286	1	2.00E + 06
145	1988	313	3	7.00E + 06
146	1988	319	1	2.00E + 06
147	1988	350	5	1.90E + 07
148	1989	5	1	3.00E + 06
149	1989	67	17	1.13E + 09
150	1989	101	6	2.02E + 08
151	1989	113	1	3.00E + 06
152	1989	121	8	4.10E + 07
153	1989	142	7	2.20E + 07
154	1989	169	2	4.00E + 06
155	1989	181	2	4.00E + 06
156	1989	206	2	1.60E + 07
157	1989	224	25	7.92E + 09
158	1989	255	5	2.90E + 07
159	1989	272	14	3.86E + 09
160	1989	292	22	1.93E + 10
161	1989	319	2	1.30E + 07
162	1989	331	8	2.21E + 09
163	1990	78	3	7.39E + 08
164	1990	88	1	3.00E + 06
165	1990	97	6	2.30E + 07
166	1990	106	7	3.30E + 07
167	1990	118	2	7.30E + 07
168	1990	128	2	3.00E + 06
169	1990	136	16	3.69E + 08

Table A17. (continued)

Event Number	Start Date		Duration (days)	Fluence >10 MeV
	Year	Day of Year		
170	1990	163	2	3.60E + 07
171	1990	207	11	1.99E + 08
172	1990	225	2	4.00E + 06
173	1991	28	5	9.00E + 07
174	1991	39	2	5.00E + 06
175	1991	56	2	5.00E + 06
176	1991	72	3	1.20E + 07
177	1991	82	17	9.75E + 09
178	1991	113	1	3.00E + 06
179	1991	130	5	1.41E + 08
180	1991	139	9	2.50E + 07
181	1991	151	21	3.25E + 09
182	1991	181	13	1.22E + 09
183	1991	238	5	1.25E + 08
184	1991	250	1	1.00E + 06
185	1991	273	3	1.40E + 07
186	1991	301	4	3.20E + 07
187	1991	363	1	1.00E + 06
188	1992	38	2	4.80E + 07
189	1992	58	1	2.00E + 06
190	1992	68	1	3.00E + 06
191	1992	75	3	9.00E + 06
192	1992	130	5	6.61E + 08
193	1992	145	1	1.00E + 06
194	1992	177	7	2.88E + 08
195	1992	219	2	7.00E + 06
196	1992	304	9	3.49E + 09
197	1992	334	1	2.00E + 06
198	1993	63	5	1.50E + 07
199	1993	71	3	2.20E + 07
200	1993	158	1	2.00E + 06
201	1994	51	3	9.95E + 08
202	1994	293	1	1.40E + 07
203	1995	293	2	1.80E + 07
204	1997	308	7	4.93E + 08
205	1998	110	6	1.62E + 09
206	1998	120	11	1.08E + 08
207	1998	168	2	3.00E + 06
208	1998	235	9	5.69E + 08
209	1998	267	2	6.00E + 06
210	1998	273	4	5.63E + 08
211	1998	292	1	2.00E + 06
212	1998	310	3	9.00E + 06
213	1998	318	4	1.38E + 08
214	1999	21	4	1.70E + 07
215	1999	114	3	1.90E + 07
216	1999	125	3	1.20E + 07
217	1999	147	1	2.00E + 06
218	1999	153	6	9.10E + 07
219	2000	49	2	5.00E + 06
220	2000	95	3	3.60E + 07
221	2000	159	6	8.40E + 07
222	2000	178	1	1.00E + 06
223	2000	195	11	1.65E + 10
224	2000	210	2	7.00E + 06
225	2000	226	1	1.00E + 06
226	2000	256	6	2.69E + 08
227	2000	290	3	1.60E + 07
228	2000	299	3	1.20E + 07
229	2000	305	2	4.00E + 06
230	2000	314	11	1.08E + 10
231	2000	329	10	4.98E + 08
232	2001	22	2	3.00E + 06
233	2001	28	3	3.40E + 07
234	2001	86	26	1.68E + 09
235	2001	117	2	5.00E + 06
236	2001	127	3	2.40E + 07
237	2001	140	2	5.00E + 06
238	2001	166	3	2.20E + 07
239	2001	222	1	6.00E + 06
240	2001	228	10	2.86E + 08

Table A17. (continued)

Event Number	Start Date		Duration (days)	Fluence >10 MeV
	Year	Day of Year		
241	2001	258	1	3.00E + 06
242	2001	267	18	8.41E + 09
243	2001	292	7	2.80E + 07
244	2001	308	9	1.52E + 10
245	2001	322	13	8.17E + 09
246	2001	360	24	7.75E + 08
247	2002	27	1	2.00E + 06
248	2002	51	1	2.00E + 06
249	2002	75	8	6.30E + 07
250	2002	107	15	2.88E + 09
251	2002	142	3	1.10E + 08
252	2002	188	4	1.50E + 07
253	2002	197	14	2.21E + 08
254	2002	226	14	3.54E + 08
255	2002	249	3	3.50E + 07
256	2002	306	1	1.00E + 06
257	2002	313	3	1.45E + 08
258	2002	354	1	1.00E + 06
259	2003	148	4	3.50E + 07
260	2003	169	3	1.60E + 07
261	2003	299	17	1.58E + 10
262	2003	324	5	2.50E + 07
263	2003	336	4	3.00E + 07
264	2004	102	2	1.80E + 07
265	2004	205	6	1.61E + 08
266	2004	214	2	3.00E + 06
267	2004	257	9	1.65E + 08
268	2004	306	2	1.90E + 07
269	2004	312	10	5.16E + 08
270	2005	15	9	3.67E + 09
271	2005	127	1	2.00E + 06
272	2005	134	3	3.81E + 08
273	2005	167	3	2.70E + 07
274	2005	195	6	1.61E + 08
275	2005	208	7	1.29E + 08
276	2005	234	2	2.27E + 08

Tables A1, A2 and A3 give the constants found applying the SEPE waiting time analysis from section 4.1 for the JPL, PSYCHIC and NOAA event lists, respectively. Tables A4–A12 give the three measures of the goodness of fit for each of the three event lists used for the waiting time results. Tables A13, A14 and A15 give the binnings used for each of the three event lists. Table A16 gives the binnings used for the SEPE duration analysis from section 4.2. Finally, Table A17 gives the complete JPL event list used.

[89] **Acknowledgments.** We would like to thank Mike Xapsos at NASA Goddard Space Flight Center for providing us with the PSYCHIC event list and information on how it was created.

[90] Amitava Bhattacharjee thanks the reviewers for their assistance in evaluating this paper.

References

- Bi, H., G. Börner, and Y. Chu (1989), Correlations in the absorption lines of the quasar Q0420-388, *Astron. Astrophys.*, 218, 19–23.
- Cane, H. V. (2005), Are there direct flare particles in large solar particle events?, in *Connecting Sun and Heliosphere: Proceedings of Solar Wind 11/SOHO 16*, edited by B. Fleck and T. H. Zurbuchen, *Eur. Space Agency Spec. Publ., ESA SP592*, 71–75.
- Carrington, R. C. (1860), Description of a singular appearance seen on the Sun on September 1, 1859, *Mon. Not. R. Astron. Soc.*, 20, 13–15.
- Dyer, C. S., K. Hunter, S. Lucas, and A. Campbell (2004), Observation of the solar particle events of October and November 2003 from CREDO and MPTB, *IEEE Trans. Nucl. Sci.*, 51(6), 3388–3393.
- Feynman, J., and S. B. Gabriel (2000), On space weather consequences and predictions, *J. Geophys. Res.*, 105(A5), 10,543–10,564.

- Feynman, J., T. P. Armstrong, L. Dao-Gibner, and S. Silverman (1990), A new interplanetary fluence model, *J. Spacecr. Rockets*, 27(4), 403–410.
- Feynman, J., G. Spitale, J. Wang, and S. Gabriel (1993), Interplanetary proton fluence model: JPL 1991, *J. Geophys. Res.*, 98(A8), 13,281–13,294.
- Feynman, J., A. Ruzmaikin, and V. Berdichevsky (2002), The JPL proton fluence model: An update, *J. Atmos. Sol. Terr. Phys.*, 64(16), 1679–1686.
- Gabriel, S. B., and G. J. Patrick (2003), Solar energetic particle events phenomenology and prediction, *Space Sci. Rev.*, 107, 56–62.
- Gopalswamy, N., S. Yashiro, G. Michalek, M. L. Kaiser, R. A. Howard, D. V. Reames, and R. L. T. Von Roseninge (2002), Interacting coronal mass ejections and solar energetic particles, *Astrophys. J.*, 572, 103–107.
- Gopalswamy, N., S. Yashiro, G. Stenborg, and R. A. Howard (2003), Coronal and interplanetary environment of large solar energetic particle events, *Proc. Int. Conf. Cosmic Rays 28th*, 3549–3552.
- Gosling, J. T. (1993), The solar flare myth, *J. Geophys. Res.*, 98(A11), 18,937–18,950.
- Ho, G. C., E. C. Roelf, G. M. Mason, D. Lario, R. E. Gold, J. E. Mazur, and J. R. Dwyer (2003), Composition variations during large solar energetic particle events, in *Solar Wind Ten*, edited by M. Velli, R. Bruno, and F. Malara, *AIP Conf. Proc.*, 679, 624–627.
- Jun, I., R. T. Swimm, A. Ruzmaikin, J. Feynman, A. J. Tytka, and W. F. Dietrich (2007), Statistics of solar energetic particle events: Fluences, durations and time intervals, *Adv. Space Res.*, 40, 304–312.
- Kahler, S. W. (2003), Energetic particle acceleration by coronal mass ejections, *Adv. Space Res.*, 32, 2587–2596.
- Kallenrode, M.-B. (2003), Current views on impulsive and gradual solar energetic particle events, *J. Phys. G Nucl. Part. Phys.*, 29, 965–981.
- Kallenrode, M.-B., and E. W. Cliver (2001), Rogue SEP events: Modeling, *Proc. Int. Conf. Cosmic Rays 27th*, 3318–3321.
- King, J. H. (1974), Solar proton fluences for 1977–1983 space missions, *J. Spacecr. Rockets*, 11(6), 401–408.
- Krucker, S., and R. P. Lin (2000), Two classes of solar proton events derived from onset time analysis, *Astrophys. J.*, 542, L61–L64.
- Kuznetsov, N. V., R. A. Nymmik, and M. I. Panasyuk (2005), Models of solar energetic particle fluxes: The main requirements and the development prospects, *Adv. Space Res.*, 36, 2003–2011.
- Laherrère, J., and D. Sornette (1998), Stretched exponential distributions in nature and economy: “Fat tails” with characteristic scales, *Eur. Phys. J. B*, 2(4), 525–539.
- Lario, D., M.-B. Kallenrode, R. B. Decker, E. C. Roelf, S. M. Krimigis, A. Aran, and B. Sanahuja (2006), Radial and longitudinal dependence of solar 4–13 MeV and 27–37 MeV proton peak intensities and fluences: Helios and IMP 8 observations, *Astrophys. J.*, 653, 1531–1544.
- Lepreti, F., V. Carbone, and P. Veltri (2001), Solar flare waiting time distribution: Varying-rate Poisson of Lévy function?, *Astrophys. J.*, 555, L133–L136.
- Mewaldt, R. A., M. D. Looper, C. M. S. Cohen, G. M. Mason, D. K. Haggerty, M. I. Desai, A. W. Labrador, R. A. Leske, and J. E. Mazur (2005), Solar-particle energy spectra during the large events of October–November 2003 and January 2005, *Proc. Int. Conf. Cosmic Rays 29th*, 101–104.
- Myagkova, I. N., M. I. Panasyuk, L. L. Lazutin, E. A. Muravieva, L. I. Starostin, T. A. Ivanova, N. N. Pavlov, I. A. Rubinshtein, N. N. Vedenkin, and N. A. Vlasova (2009), December 2006 solar extreme events and their influence on the near-Earth space environment: “Universitetskij-Tatiana” satellite observations, *Adv. Space Res.*, 43, 489–494, doi:10.1016/j.asr.2008.07.019.
- Nolan, J. P. (2009), *Stable Distributions: Models for Heavy Tailed Data*, Birkhäuser, Boston, Mass.
- Nymmik, R. A. (1999), Probabilistic model for fluences and peak fluxes of solar energetic particles, *Radiat. Meas.*, 30(3), 287–296.
- Reames, D. V. (1999), Particle acceleration at the Sun and in the heliosphere, *Space Sci. Rev.*, 90, 413–491.
- Reames, D. V. (2004), Solar energetic particle variations, *Adv. Space Res.*, 34, 381–390.
- Reinard, A. A., and M. A. Andrews (2006), Comparison of CME characteristics for SEP and non-SEP related events, *Adv. Space Res.*, 38, 480–483.
- Rosenqvist, L., A. Hilgers, H. Evans, E. Daly, M. Hapgood, R. Stamper, R. Zwickl, S. Bourdarie, and D. Boscher (2005), Toolkit for updating interplanetary proton-cumulated fluence models, *J. Spacecr. Rockets*, 42(6), 1077–1090.
- Shea, M. A., D. F. Smart, K. G. McCracken, G. A. M. Dreschhoff, and H. E. Spence (2006), Solar proton events for 450 years: The Carrington event in perspective, *Adv. Space Res.*, 38, 232–238.
- Tytka, A. J., W. F. Dietrich, and P. R. Bobery (1997), Probability distributions of high-energy solar-heavy-ion fluxes from IMP-8: 1973–1996, *IEEE Trans. Nucl. Sci.*, 44(6), 2140–2149.

- Wang, R., and J. Wang (2004), Coronal mass ejections and the largest solar energetic particle events, *Proc. Int. Astron. Union*, 2004, 379–380.
- Weron, R. (1996), On the Chambers-Mallows-Stuck method for simulating skewed stable random variables, *Stat. Probab. Lett.*, 28, 165–171.
- Wheatland, M. S. (2000), The origin of the solar flare waiting-time distribution, *Astrophys. J.*, 536, L109–L112.
- Wheatland, M. S. (2003), The coronal mass ejection waiting-time distribution, *Sol. Phys.*, 214, 361–373.
- Xapsos, M. A., G. P. Summers, and E. A. Burke (1998), Probability model for peak fluxes of solar proton events, *IEEE Trans. Nucl. Sci.*, 45(6), 2948–2953.
- Xapsos, M. A., G. P. Summers, J. L. Barth, E. G. Stassinopoulos, and E. A. Burke (1999), Probability model for worst case solar proton event fluences, *IEEE Trans. Nucl. Sci.*, 46(6), 1481–1485.
- Xapsos, M. A., G. P. Summers, J. L. Barth, E. G. Stassinopoulos, and E. A. Burke (2000), Probability model for cumulative solar proton event fluences, *IEEE Trans. Nucl. Sci.*, 47(3), 486–490.
- Xapsos, M. A., C. Stauffer, G. B. Gee, J. L. Barth, E. G. Stassinopoulos, and R. E. McGuire (2004), Model for solar proton risk assessment, *IEEE Trans. Nucl. Sci.*, 51(6), 3394–3398.
- Xapsos, M. A., C. Stauffer, J. L. Barth, and E. A. Burke (2006), Solar particle events and self-organized criticality: Are deterministic predictions of events possible?, *IEEE Trans. Nucl. Sci.*, 53(4), 1839–1843.

S. B. Gabriel and P. T. A. Jiggins, Astronautics Research Group, University of Southampton, Southampton SO17 1BJ, UK. (piers.jiggins@soton.ac.uk)